

AD-751 528

STRESS CORROSION CRACKING OF TITANIUM
ALLOYS IN METHANOLIC AND OTHER MEDIA

C. M. Chen, et al

Air Force Materials Laboratory
Wright-Patterson Air Force Base, Ohio

March 1972

DISTRIBUTED BY:

NTIS

National Technical Information Service
U. S. DEPARTMENT OF COMMERCE
5285 Port Royal Road, Springfield Va. 22151

AD 751528

AFML-TR-71-232



STRESS CORROSION CRACKING OF TITANIUM ALLOYS IN METHANOLIC AND OTHER MEDIA

C. M. CHEN

OHIO STATE UNIVERSITY

H. B. KIRKPATRICK

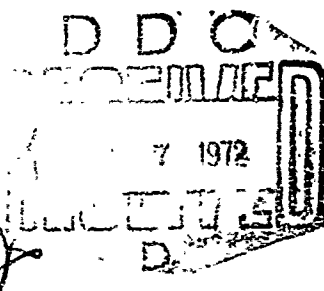
H. L. GEGEL

AIR FORCE MATERIALS LABORATORY

TECHNICAL REPORT AFML-TR-71-232

MARCH 1972

Reproduced by
NATIONAL TECHNICAL
INFORMATION SERVICE
U S Department of Commerce
Springfield VA 22151



Approved for public release; distribution unlimited.

AIR FORCE MATERIALS LABORATORY
AIR FORCE SYSTEMS COMMAND
WRIGHT-PATTERSON AIR FORCE BASE, OHIO

NOTICE

When Government drawings, specifications, or other data are used for any purpose other than in connection with a definitely related Government procurement operation, the United States Government thereby incurs no responsibility nor any obligation whatsoever; and the fact that the government may have formulated, furnished, or in any way supplied the said drawings, specifications, or other data, is not to be regarded by implication or otherwise as in any manner licensing the holder or any other person or corporation, or conveying any rights or permission to manufacture, use, or sell any patented invention that may in any way be related thereto.

Copies of this report should not be returned unless return is required by security considerations, contractual obligations, or notice on a specific document.

AIR FORCE: 25-5-72/150

**STRESS CORROSION CRACKING OF TITANIUM
ALLOYS IN METHANOLIC AND OTHER MEDIA**

*C. M. CHEN
H. B. KIRKPATRICK
H. L. GEGEL*

Approved for public release; distribution unlimited.

1

FOREWORD

This program was initiated under Project 7353, "Characterization of Solid Phase and Interphase Phenomena in Crystalline Substances", and Task No. 735302, "Correlation of Physical and Mechanical Properties of Metals and Ceramics", during the period April 1969 through September 1970.

This research was done in the Advanced Metallurgical Studies Branch of the Metals and Ceramics Division, Air Force Materials Laboratory, Wright-Patterson Air Force Base, Ohio 45433. The principal investigators were Dr. C.M. Chen of Ohio State University and Dr. H.B. Kirkpatrick (AFML/LLS); the coauthor was Dr. H.L. Gegel (AFML/LLS).

This report was submitted by the authors in April 1971.

This technical report has been reviewed and is approved.

C.T. Lynch
C. T. LYNCH
Chief, Advanced Metallurgical
Studies Branch
Metals and Ceramics Division
Air Force Materials Laboratory

UNCLASSIFIED

Security Classification

DOCUMENT CONTROL DATA - R & D		
<i>(Security classification of title, body of abstract and indexing annotation must be entered when the overall report is classified)</i>		
1. ORIGINATING ACTIVITY (Corporate author) Air Force Materials Laboratory Wright-Patterson Air Force Base, Ohio 45433		2a. REPORT SECURITY CLASSIFICATION UNCLASSIFIED
		2b. GROUP
3. REPORT TITLE STRESS CORROSION CRACKING OF TITANIUM ALLOYS IN METHANOLIC AND OTHER MEDIA		
4. DESCRIPTIVE NOTES (Type of report and inclusive dates) April 1969 through September 1970		
5. AUTHOR(S) (First name, middle initial, last name) C. M. Chen; H. B. Kirkpatrick; H. L. Gegel		
6. REPORT DATE March 1972	7a. TOTAL NO. OF PAGES 68	7b. NO. OF REFS 37
8a. CONTRACT OR GRANT NO.		9a. ORIGINATOR'S REPORT NUMBER(S)
b. PROJECT NO. 7353		AFML-TR-71-232
c. Task No. 735302		9b. OTHER REPORT NO(S) (Any other numbers that may be assigned this report)
d.		
10. DISTRIBUTION STATEMENT Approved for public release; distribution unlimited.		
11. SUPPLEMENTARY NOTES		12. SPONSORING MILITARY ACTIVITY Air Force Materials Laboratory Wright-Patterson Air Force Base, Ohio 45433
13. ABSTRACT Results are given of a systematic survey of the stress-corrosion cracking behavior of titanium and certain of its alloys in such environments as pure organic liquids, organic liquid-bromine mixtures, methanol-water-acid mixtures, methanol vapor, and liquid mercury. Stress-corrosion behavior is measured by time-to-failure under static tensile load and by reduction in ultimate elongation under dynamic tension. The effects are described of such variables as water concentration, bromine concentration, applied electrical potential, and strain rate. Depending on the circumstances, mechanical failure appears to be associated with different processes or mechanisms such as anodic dissolution at grain boundaries, hydrogen embrittlement, corrosive reactions between titanium and bromine or methanol, catalytic dehydrogenation of methanol, or stress sorption. Details of illustrations in this document may be better studied on microfiche.		

DD FORM 1 NOV 61 1473

(a)

UNCLASSIFIED

Security Classification

UNCLASSIFIED

Security Classification

14	KEY WORDS	LINK A		LINK B		LINK C	
		ROLE	WT	ROLE	WT	ROLE	WT
	Stress Corrosion Titanium Alloys Methanol						

(b)

UNCLASSIFIED

Security Classification

ABSTRACT

Results are given of a systematic survey of the stress-corrosion cracking behavior of titanium and certain of its alloys in such environments as pure organic liquids, organic liquid-bromine mixtures, methanol-water-acid mixtures, methanol vapor, and liquid mercury. Stress-corrosion behavior is measured by time-to-failure under static tensile load and by reduction in ultimate elongation under dynamic tension. The effects are described of such variables as water concentration, bromine concentration, applied electrical potential, and strain rate. Depending on the circumstances, mechanical failure appears to be associated with different processes or mechanisms such as anodic dissolution at grain boundaries, hydrogen embrittlement, corrosive reactions between titanium and bromine or methanol, catalytic dehydrogenation of methanol, or stress sorption.

TABLE OF CONTENTS

SECTION		PAGE
I	Introduction	1
II	Experimental Procedures	3
III	Results	4
	1. Methanol-Water-Hydrochloric Acid Mixtures at the Corrosion Potential	4
	2. Methanol-Water-Hydrochloric Acid Mixtures Under Anodic or Cathodic Polarization	8
	3. Failure of Unalloyed (RMI-70) Titanium and of Several Alloys in "Nonaqueous" Media	11
	a. Methanol, Liquid, Absolute, As Received	13
	b. Absolute Methanol + CaO Desiccant	13
	c. Methanol Vapor	13
	d. "Pure" Solvents	16
	e. Methanol-Carbon Tetrachloride Mixtures	16
	f. Solvents Containing 1/2% Bromine	17
	g. Methanol-Bromine Solutions	18
	4. Cracking of Ti 8Al-1Mo-1V and Ti 6Al 4V Alloys by Liquid Mercury	20
IV	Summary	21
	References	22

Preceding page blank

ILLUSTRATIONS

FIGURE	PAGE
1a. Specimen Configurations	25
1b. Cell for Straining Electrode Tests	26
1c. Cell for Stress Corrosion Bend Tests	27
2a. Failure Time vs Water Content at Corrosion Potential	28
2b. Elongation vs Water Content; CH ₃ OH + 0.166% HCl + H ₂ O (Tensile Direction Parallel to Rolling Direction; Strain Rate 0.005 cm/min)	29
3. Corrosion Potential vs Water Content; CH ₃ OH + 0.166% HCl + H ₂ O (No Applied Load)	30
4. Corrosion Potential vs Elongation in CH ₃ OH + 0.166% HCl + H ₂ O	31
5a. Effect of Strain Rate on Corrosion Potential vs Strain in CH ₃ OH + 0.166% HCl + 0.28% H ₂ O	32
5b. Effect of Strain Rate on Corrosion Potential vs Strain in CH ₃ OH + 0.166% HCl + 0.99% H ₂ O	33
6. Half-Range of Scatter in Failure Time vs Average Failure Time	34
7. Failure Time vs Polarization Potential in CH ₃ OH + 0.166% HCl + 0.99% H ₂ O	35
8. Effect of Water Content on the Polarization Curves in CH ₃ OH + 0.166% HCl + H ₂ O (Scanning rate 25 mV/min)	36
9. Pitting and Crack Formation of Ti-6Al-4V Alloy in CH ₃ OH + 0.17% HCl + 1% H ₂ O, Under Polarization of +450 mV (SHE)	37

ILLUSTRATIONS (CONTD)

FIGURE	PAGE
10. Corrosion Products on External and Fracture Surfaces of Ti-6Al-4V Fractured in $\text{CH}_3\text{OH} + 0.17\% \text{HCl} + 1\% \text{H}_2\text{O}$ (Carbon Replica; X2,350) (a) External Surface; (b) Fracture Surface; (c) Electron Diffraction Pattern of Corrosion Product (TiCl_3)	38
11. Effect of Polarization Potential on Elongation	39
12. Transition Potential vs Water Content	40
13a. Effect of Strain Rate on Specimen Elongation at +350 mV (SHE)	41
13b. Effect of Strain Rate on Specimen Elongation at +50 mV (SHE)	42
14. Stress-Strain Curves of Ti-6Al-4V in Air and in Absolute Reagent Grade Methanol (0.015% H_2O)	43
15. Transgranular Stress Corrosion Cracking of Heat-Treated β -III Alloy in Methanol Vapor	44
16a. Failure Time vs Bromine Concentration Titanium 8-1-1	45
16b. Failure Time vs Bromine Concentration; Heat-Treated β -III	46
17. Weight Loss vs Bromine Concentration; Titanium 8-1-1	47
18. Stress Corrosion Cracking of Ti-8Al-1Mo-1V Alloy in CH_3OH ; 0.5% Bromine Solution (X50)	48
19. Intergranular Corrosion of Unalloyed Titanium (RMI70) in Bromine-Methanol Solution (1% Br_2 ; 68-Hour Exposure; No External Stress; X300)	49
20. Grain Boundary Corrosion Near Center of Heat-Treated β -III Alloy Specimen in Bromine-Methanol Solution (0.05% Br_2 ; 164 Hours; No External Stress; X210)	50

ILLUSTRATIONS (CONTD)

FIGURE		PAGE
21.	Stress Corrosion Cracking of Heat-Treated β -III Alloy in Bromine-Methanol Solution (0.5%Br ₂ ; X50)	51
22.	Stress Corrosion Cracking From Residual Stress at Edge of β -III Specimen (0.05%Br ₂ ; X150)	52
23.	Transgranular Cracking of Highly Stressed β -III Alloy in Bromine-Methanol Solution (Note relationship of crack direction to slip lines caused by plastic deformation.)	53
24.	Stress Corrosion Cracking of Heat-Treated β -III Alloy in CH ₃ OH + 0.17%HCl + 0.28%H ₂ O (X100)	54

SECTION I

INTRODUCTION

Since Fontana (Reference 1) reported in 1956 on the intergranular cracking of Ti-5Al-2 1/2 Sn alloy in 10% hydrochloric acid, and Brown (Reference 2) showed in 1966 that Ti-8Al-1Mo-1V failed readily in 3 1/2% sodium chloride solution, there have been many studies of various aspects of the stress corrosion behavior of titanium (References 3 through 6) and its alloys (References 7 through 12). The failure of a titanium alloy pressure vessel upon being pressurized with methyl alcohol in 1966, led to a surge of investigations of the stress corrosion cracking of titanium alloys by alcohols, halogenated hydrocarbons, and other organic liquids (References 13 through 23).

While both practical and academic concern with the problem of "alcohol cracking" seem to have declined considerably since the discovery that it could be inhibited by the presence of water, water-halogen-organic liquid systems continue to be interesting for purposes of mechanism investigation. By suitable choice of organic liquid, variation of water and halogen concentrations, and application of potentiostatic techniques, insight may be gained as to the roles played in the failure process by such effects as anodic dissolution, cathodic embrittlement, halogen or halide-ion attack, metal-organic reactions, and stress-sorption cracking.

This report describes some results obtained in a systematic survey of the cracking behavior of titanium alloys in organic-halogen-water mixtures, as affected by variations in solution composition and electrical potential.

SECTION II

EXPERIMENTAL PROCEDURES

Smooth Tensile and bend specimens of the dimensions given in Figure 1a were prepared from rolled Ti-6Al-4V and Ti-8Al-1Mo-1V sheet material. In the case of β -III alloy and unalloyed titanium, the U-bend specimens had thicknesses of 0.13 mm and 0.64 mm respectively, rather than 0.26 mm. Tensile specimens were placed in the test cell illustrated in Figure 1b and were strained during testing with an Instron machine at strain rates ranging from 0.005 to 0.5 cm/min (0.36-36%/min). Bend specimens were restrained in short lengths of glass tubing as is shown in Figure 1c. Cylindrical platinum counter electrodes surrounded the specimens and Luggin probes were placed in the cell as in Figures 1b and c. A zoom stereo microscope was used in conjunction with a closed circuit TV camera to observe crack propagation in the bend specimens.

SECTION III

RESULTS

1. METHANOL-WATER-HYDROCHLORIC ACID MIXTURES AT THE CORROSION POTENTIAL

While the inhibiting effect of water on alcohol cracking has been reported a number of times (References 4 and 20), the results of varying the water concentration were also studied in this survey to compare the effects of such variation on (1) the failure time of U-bend specimens; (2) the ultimate elongation of tensile specimens; (3) the corrosion potential; and (4) the polarization behavior.

Figure 2a shows the effect of water content in X w/o CH_3OH -0.17 w/o HCl -Y w/o H_2O mixtures upon time to failure of U-bend specimens of Ti-6Al-4V alloy. Similarly, Figure 2b shows the effect of water content upon the ultimate elongation of un-notched dynamically strained tensile specimens of the same alloy (as-received condition). (In these figures, zero water content refers to reagent grade absolute methanol having a water content of about 0.05%, which is taken into account. Fracture behavior in this absolute methanol was not significantly different from that in air.) In both cases, water concentrations in the range 0.3 to 0.6% had the maximum effect, i.e., minimum times to failure and minimum elongation at fracture. Outside this range the fracture behavior

changed rapidly to that characteristic of air or pure solvent. The effect of increasing water concentration has been attributed to the formation of passive oxide films which interfere with crack initiation or propagation (References 4 and 20).

Figure 3 shows the effect of water concentration in the CH_3OH -0.17% HCl - H_2O mixtures upon the open circuit corrosion potential (SHE) of 6-4 alloy. It can be seen that in the region of greatest stress corrosion cracking (SCC) susceptibility, i.e., 0.2 to 0.6%, the corrosion potential tends to shift in the anodic direction as the water content is increased. Above 0.6% the potential becomes more or less independent of the water content.

Figure 4 illustrates the variation of corrosion potential with elongation of the 6-4 specimen, under tensile loading at 0.005 cm/min (0.36%/min), in solutions having different water contents. Potentials are observed to be altered by strain in the anodic direction at water contents of 0.8% and lower, and in the cathodic direction at higher values.

Figures 5 a and b show the effects of straining, at different strain rates, on the corrosion potentials in solutions having water contents of 0.28% and 0.99%, respectively. In the 0.99% solution, the strain rate has little effect on the behavior of the corrosion potential; in the

0.28% solution, increasing the strain rate increases the cathodic shift of the potential with strain, and also increases the ultimate elongation to values typical of those in air.

Sedricks and coworkers (References 4,5,21 and 22) have discussed the effects of water on the SCC behavior of titanium in methanol-bromine and methanol-iodine solutions, the inhibiting effect being attributed to the formation of passive, protective films at sufficiently high water concentrations. Also Haney (References 20 and 24) in the case of Ti-13V-11Cr-3Al alloy in $\text{CH}_3\text{OH-NaCl-H}_2\text{O}$ solutions, has reported susceptibility to be at a maximum just before the onset of passivity. The present results may be rationalized, at least partially, by similar considerations. Thus the metal surface can be thought of as covered by a protective oxide film containing defective portions which act as sites of anodic dissolution and crack formation. The remaining oxide-covered surface acts as a cathode. The defective parts may be preexisting in the air formed oxide film, or created during strain of the specimen. It would appear that in the presence of water such defects become repaired or passivated. As the water concentration is increased from about 0.25%, the number of anodic defective sites and the anodic current are reduced, and so the corrosion potential shifts in the anodic direction, as seen in Figure 3. At water concentrations

above a rather critical value of about 0.8%, the repair or passivation is complete, cracking is inhibited, and the potential becomes independent of water content, again as in Figure 3. On this model it would be anticipated that upon straining the specimen, the anodic current should be increased, due to the creation of defects in the oxide film or to the exposure of fresh metal surface, and the corrosion potential should shift in the cathodic direction. As can be seen in Figures 4 and 5, such a cathodic shift is in fact observed when the water content is above about 0.8% and/or the strain rate greater than 0.1 cm/min. Below these values the corrosion potential shift is in the anodic direction, which is difficult to interpret except perhaps on the basis that the combination of dynamic strain and incompletely passivated surface introduces a new anodic reaction of higher EMF.

Upon examination of the data on time to failure as a function of water content in $\text{CH}_3\text{OH}-0.17\%\text{HCl}-\text{H}_2\text{O}$ solutions, there appears to be a surprisingly well defined relationship between the magnitude of a failure time and the range of scatter in its values. This is illustrated in Figure 6, which is a log-log plot of average failure time at different water contents against the corresponding half-range of scatter. The same linear relationship appears to hold for unalloyed

titanium, Ti-6Al-4V, Ti-8Al-1Mo-1V, and β -3 alloy. Whether the relationship has any fundamental significance remains to be seen. However it does imply that under conditions of moderate to low SCC susceptibility, cracking behavior becomes extremely unpredictable.

2. METHANOL-WATER-HYDROCHLORIC ACID MIXTURES UNDER ANODIC OR CATHODIC POLARIZATION

Figure 7 shows the effect of applied anodic and cathodic potentials on the stress corrosion failure times of Ti-6Al-4V U-bend specimens in CH_3OH -0.17% HCl -0.99% H_2O solutions. Somewhat similar measurements have been reported elsewhere (References 5 and 12), but the present results are included here for purposes of comparison and completeness of presentation. Note that while this water concentration of 0.99% would normally prevent cracking, the application of anodic potentials above about 200 mV (SHE) leads to rapid failure. In the potential range from about +200 to -200 mV, the alloy apparently becomes insusceptible to SCC, with susceptibility returning at higher cathodic potentials, around -600 mV.

Figure 8 gives the anodic and cathodic polarization curves for 6-4 alloy in methanol-0.17% hydrochloric acid-water mixtures, having various water contents. It can be seen that the effect of the water is enormously greater on the anodic current than on the cathodic. Thus the inhibiting

effect of water on the SCC is apparently associated with the great reduction in anodic current. Similar results have been reported by Sedricks, et al., for unalloyed titanium and Ti-Al alloys (Reference 4), by Levy and Seitz for Ti-8Al-1Mo-1V (Reference 12) and by Haney, et al. (Reference 24), although generally at much higher water contents.

Under anodic polarization, crack formation takes place by a pitting mechanism. In the case of Ti 6-4 U-bend specimens in CH_3OH -0.17%-HCl-1% H_2O water, pits are observed to form at potentials of about +300 mV (SHE), or higher, the number of pits increasing rapidly with potential. Under microscopic observation, cracks are seen to originate at the pits and grow laterally perpendicular to the direction of tensile stress. (See Figure 9.) Fontana, et al. (Reference 25) have reported that in the case of 6-4 alloy in CH_3OH - H_2O -NaCl solutions, the pits originate by selective attack of β grains and along the α - β interface. Fontana (Reference 25) has reported observing, by light microscopy, black corrosion product in the pits, and the present authors have also observed such material both in the pits and on the fracture surfaces, as shown in Figure 10. The corrosion product was identified by electron diffraction as TiCl_3 (Figure 10).

The effects of anodic and cathodic polarization on the ultimate elongation of dynamically strained tensile specimens

of Ti 6-4 are illustrated in Figure 11, for various water concentrations. It can be seen that at any particular water content, there is a fairly definite potential associated with the transition from insusceptible to susceptible, or embrittled, behavior. (The average elongation at fracture in air was about 7%.) As the water content is increased, the transition potential becomes increasingly anodic. In Figure 12, this transition potential is plotted as a function of water concentration for comparison with the corrosion potential (shaded area). At about 0.6 to 0.7% water, the corrosion potential becomes less than the potential necessary to produce embrittlement.

The effect of strain rate on ultimate elongation, under anodic (+350 mV SHE) and slightly cathodic (+50 mV SHE) polarization relative to the corrosion potential at 0.42% H_2O , is illustrated in Figures 13a and b. At this level of cathodic polarization, the alloy is not embrittled and susceptible to SCC and the normal elongations typical of fracture in air were observed at all the strain rates employed. With anodic polarization and embrittlement, the ultimate elongation is very sensitive to the strain rate, increasing rapidly with rate in the range 0.005 to 0.020 cm/min. Above about 0.050 cm/min, the normal fracture process apparently becomes faster than the stress corrosion cracking, and elongations

only slightly less than that in air are observed, more or less independent of strain rate.

As has been stated by other workers (References 4, 12, and 20) it is concluded that, when the water content of the methanol is in the range of about 0.015 to 0.8%, stress corrosion cracking of commercial Ti-6Al-4V alloy takes place by an electrochemical anodic dissolution process, under conditions of anodic polarization or at the corrosion potential.

Crack initiation appears to occur at relatively anodic defect sites in the metal surface or surface oxide film, on β -grains and α - β interfaces. High cathodic polarization will also produce stress corrosion failure, but presumably by a different mechanism, perhaps hydrogen embrittlement.

3. FAILURE OF UNALLOYED (RMI-70) TITANIUM AND OF SEVERAL ALLOYS IN "NONAQUEOUS" MEDIA

In addition to the above described work in the CH_3OH - HCl - H_2O system, a number of failure time measurements of U-bend specimens were made in "pure" (as received) solvents and solvents + bromine, to note the SCC behavior in the relative absence of water, and effects due to reactions with solvent or the bromine. These results are shown in Table I.

TABLE I

FAILURE TIMES OF U-BEND SPECIMENS OF AS-RECEIVED TITANIUM ALLOYS IN VARIOUS MEDIA

SOLUTION	MATERIAL				
	Ti-8Al-1Mo-1V	Ti-6Al-4V	RMI-70 (Unalloyed Ti)	Ti-11.5Mo-6Zr -4.5Sn (β -III)	β -III (heat- treated)
Diethyl Ether	T=1 N.F.=300h	T=1 N.F.=300h	T=1 N.F.=300h	T=1 N.F.=300h	
Diethyl Ether +0.5% Br_2	T=6 F=104m, 9m, 5m 120m, 12m, 11m	T=1 F=20h	T=1 N.F.=300h	T=1 F=96h	
Benzene	T=1 N.F.=300h	T=1 N.F.=300h	T=1 N.F.=300h	T=1 N.F.=300h	
Benzene + 0.5% Br_2	T=2 F=65m, 100m	T=1 N.F.=300h	T=1 N.F.=300h	T=1 N.F.=300h	
Carbon Tetrachloride	T=3 N.F.=30d	T=3 N.F.=30d	T=3 N.F.=30d	T=3 N.F.=30d	
Carbon Tetrachloride + 0.5% Br_2	T=10 F=3h, 10h, 20h 23h, 30d N.F.=5; 30d	T=2 N.F.=300h	T=2 N.F.=300h	T=2 N.F.=300h	T=3 F=1.5h, 2h, 3h
Methanol	T=8 F=1.5h, 3h 101h, 20d, 20d N.F.=3; 30d	T=8 N.F.=300h	T=4 N.F.=300h	T=6 F=44h, 60h N.F.=4; 200h	
Methanol + CaO	T=4 F=2h, 11h, 81h N.F.=1; 300h	T=4 F=144h, 50h 170h, 40h	T=2 N.F.=300h	T=6 F=40h, 78h, 30h 58h, 20h, 55h	
Methanol Vapor (+CaO)	T=4 F=11h, 80h, 125h N.F.=1; 300h	T=3 F=140h, 164h 200h	T=3 F=63h, 164h N.F.=1; 300h	T=4 F=15h, 39h, 39h N.F.=1; 300h	T=3 F=39h, 60h 290h

NOTE: Tensile stress direction perpendicular to rolling direction.

T = total number of specimens tested
 F = observed times of failure
 N.F. = number not failed after stated time
 m = minutes
 h = hours
 d = days

The following is a summary of the results shown in the Table.

a. Methanol, Liquid, Absolute, As Received

The as-received methanol contains about 0.015% water. In this medium failures were observed in the 8-1-1 and β -III alloys after periods of a few hours to several days. The 6-4 alloy and the unalloyed RMI-70 titanium had no failures after 300 hours. It may be seen from Figure 14 that for the 6-4 alloy, the stress-strain curve in methanol is about the same as in air, having a slightly higher slope and a slightly lowered ultimate elongation. Gegel, Kirkpatrick, and Swinning (Reference 11) and Gegel and Fujishiro (Reference 26) have reported that when 6-4 was fractured in methanol, TiH_2 was detected on the fracture surfaces by electron diffraction. Whether such hydride formation is causally related to SCC, has yet to be established.

b. Absolute Methanol + CaO Desiccant

Additional measurements were made with methanol containing CaO to lower the water content still further. Under this condition, failures were observed in all the alloys, but not in the unalloyed titanium after 300 hours.

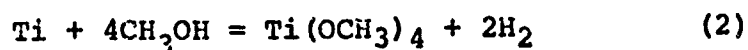
c. Methanol Vapor

Specimens (U-bend) were exposed to methanol vapor by being placed in a desiccator along side a beaker containing liquid CH_3OH over CaO. There was also CaO in the desiccant

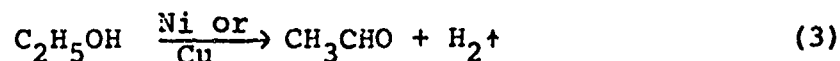
chamber. Specimen failure occurred in the majority of cases for all three alloys and for the unalloyed metal, and it is interesting that methanol vapor is the only "nonaqueous" medium in which all the metals tested were susceptible. Moreover, generally speaking, the susceptibility to cracking appears to be considerably greater in the vapor than in the as-received liquid absolute alcohol. Except for the unalloyed titanium, the vapor susceptibility is comparable to that in the liquid dried with CaO. Ambrose and Kruger (Reference 23) have reported similar results in the case of unalloyed titanium and Ti-8Al-1Mo-1V and have also reported the detection of formaldehyde in the reaction vessel. On this basis they discussed the possible connection of the stress corrosion cracking with the catalytic dehydrogenation of methanol on the metal surface, according to the reaction.



Since the reaction produces hydrogen, it is tempting to regard the cracking as resulting from hydrogen embrittlement, but on the basis of their results Ambrose and Kruger advance several arguments against this. Reaction 1 is not the only one capable of producing hydrogen. Gegel, Kirkpatrick, and Swinning (Reference 11) suggested that titanium might react with anhydrous methanol to form hydrogen and titanium methoxide:



Subsequently, Leith, Hightower, and Harkins (Reference 27) demonstrated the occurrence of such a reaction between anhydrous methanol vapor and vacuum-deposited films of titanium, in the temperature range 120 to 150°C. The addition of water vapor inhibited the reaction and the addition of hydrogen chloride gas greatly increased the rate of disappearance of the metal film, even at room temperature. The similarity of these effects of water and hydrogen chloride to their effects in the aqueous alcohol solutions, plus the fact that Reaction 2 is a "corrosion" reaction involving consumption of the metal, would seem to favor Reaction 2 as the one involved in cracking by the methanol vapor, rather than the catalytic Reaction 1. On the other hand, given the formaldehyde formation reported by Ambrose and Kruger, it would seem that that Reaction 1 actually occurred under their conditions, i.e., U-bend specimens highly strained, probably past the yield point. A dehydrogenation reaction similar to Reaction 1 occurs with ethanol in the presence of nickel or copper catalysts, forming acetaldehyde:



Kishimoto (Reference 28) and Uhara, et al. (Reference 29), have shown that the active sites of the catalysis in this reaction are lattice defects, i.e., vacancies or termination points of dislocation lines at the metal surface. Thus, if

the U-bend specimens of Ambrose and Kruger were more highly strained than the films of Leith, Hightower, and Harkins, as seems likely, Reaction 1 might have been favored over Reaction 2. Heterogeneous catalysis processes are known to be sensitive to crystallographic orientation and it may be significant that when heat-treated β -III alloy was exposed to methanol vapor, the transgranular cracks appeared to lie along {001} planes, as shown in Figure 15.

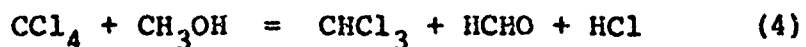
d. "Pure" Solvents

U-bend specimens were exposed to as-received reagent grade benzene, diethyl ether, and carbon tetrachloride. No failures were observed in these environments after 300 hours in the case of benzene and ether, and after 30 days in carbon tetrachloride. However carbon tetrachloride has been reported to accelerate crack growth in notched precracked specimens of Ti-8Al-1Mo-1V (References 30 and 31).

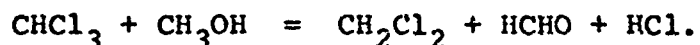
e. Methanol-Carbon Tetrachloride Mixtures

Aluminum alloys containing copper or zinc have been reported to be severely corroded by mixtures of carbon tetrachloride and methanol, more rapidly than by the individual constituents (References 32 and 33). To see if there was a similar effect in the stress corrosion of titanium, specimens of unalloyed RMI-70 titanium were exposed to mixtures of as-received solvents in the range 10 to 30% by volume CCl_4 . In these mixtures, failures occurred after 100 to 200 hours whereas there were no failures after 300 hours in methanol and

after 30 days in carbon tetrachloride. Thus there did appear to be some increase of susceptibility. In this case the failures were presumably associated with the reactions:



and



f. Solvents Containing 1/2% Bromine

To examine nonaqueous corrosion and the effects of type of solvent on SCC susceptibility, failure time tests were carried out in as-received benzene, ethyl ether, and carbon tetrachloride containing 1/2% dissolved bromine. Results are shown in Table I. In the carbon tetrachloride solution, failures occurred only with part of the 8-1-1 specimens and with heat-treated β -III alloy. In the benzene solution, 8-1-1 specimens failed fairly rapidly but there were no failures of the other alloys or the unalloyed titanium. In the ether-bromine solution there was a slow failure of as-received β -III and rapid failure of 8-1-1. In the case of the 8-1-1 alloy there was noticed a reduction in time to failure as successive specimens were tested in the same ether-bromine solution. Thus in Table I, the first specimen failed in 104 minutes. After the solution had stood overnight, succeeding specimens failed in 9 and then 5 minutes. Upon repeating the test, after the first specimen had failed at 120 minutes, a new specimen was put in immediately and failed in 12 minutes,

and the next, in 11. This shortening of failure time thus seems to be due to accumulation of some reaction product in the solution, rather than an aging effect observed by Cocks, et al., in methanol-bromine solutions and attributed to a photochemical reaction between bromine and methanol vapor (Reference 34).

g. Methanol-Bromine Solutions

Failure times in methanol-bromine solutions, as a function of bromine concentration, are shown in Figure 16a for Ti-8Al-1Mo-1V and in Figure 16b for β -III alloy heat-treated to produce all β -phase. Note that bromine concentrations as low as $5 \times 10^{-5}\%$ (by volume) still produce rapid failures. Also the curve for 8-1-1 shows a minimum at 0.05 to 0.5%. The Ti-6Al-4V and unalloyed titanium show similar tendencies except that failure times are longer and the minima are not conspicuous. The minimum is presumably due to increased general corrosion and crack blunting at higher bromine concentrations. For purposes of comparison, weight loss measurements of Ti 8-1-1 as a function of time were made in the bromine solutions, the results being shown in Figure 17. It is interesting that in the $5 \times 10^{-5}\%$ solution, a weight loss on the order of a microgram or less per cm^2 of specimen surface could still cause failure in about five minutes.

In the case of the 8-1-1 alloy, some observations were made of the effect of the relative orientation of the tensile

and rolling directions on crack behavior, as illustrated in Figure 18. When the tensile direction was perpendicular to the rolling direction, the cracks followed the rolling direction very closely; when the tensile direction was at 45° to that of rolling, the cracks deviated from the rolling direction by about 15 to 20° ; and when the tensile direction was parallel to the rolling direction, the cracks were oriented both in the rolling direction and at about 15 to 20° to it. Fager and Spurr (Reference 35) have shown that in the rolled material the (0001) planes are preferentially oriented normal to the plate surface and parallel to the rolling direction. Therefore, orientation of the crack direction at 15 to 20° to that of rolling, means that the crack planes approximately follow the $(10\bar{1}7)$ or $(10\bar{1}8)$ cleavage planes (References 35 and 36).

In the case of unalloyed titanium in the methanol-bromine solutions, the "pure" corrosion reaction with no applied stress is intergranular, as shown in Figure 19. At moderate stress, both the corrosion and the stress corrosion cracking were intergranular. However at higher stresses, a small amount of transgranular cracking was observed.

With β -III alloy heat-treated to produce all β -phase, the corrosion with no applied stress was also intergranular, Figure 20. When stress is applied, the stress corrosion cracking is mixed inter- and transgranular, being mostly

intergranular when the bromine concentration is 0.5% or greater (Figure 21). At lower bromine concentrations the stress corrosion cracking appears to be largely transgranular, as illustrated in Figures 22 and 23. The stress corrosion cracking of heat-treated β -III is also mixed inter- and transgranular in methanol-hydrochloric acid-water mixtures as shown in Figure 24.

4. Cracking of Ti 8Al-1Mo-1V and Ti 6Al-4V Alloys by Liquid Mercury

Chen and Kirkpatrick (Reference 37) have reported a very marked reduction in time-to-failure of Ti 8-1-1 in liquid mercury by ultrasonic oscillation, and with Ti 6-4 to a somewhat lesser extent. On the basis of the rapidity of the failure and the wetting behavior of the mercury on the fresh fracture surfaces, they attributed the failure to a stress-sorption mechanism.

SECTION IV

Summary

On the basis of the work reported here, in conjunction with that of others, the stress corrosion failure of titanium and its alloys appears to be connected with different chemical or physical processes, depending on the medium. For the media studied, these processes seem to be as follows:

a. In methanol-water-halide solutions, at the corrosion potential or under anodic polarization, an anodic dissolution of metal along the grain boundaries, with crack initiation taking place at defect sites in the protective oxide film or at corrosion pits caused by chloride ion attack;

b. In methanol-water-halide solutions at high cathodic polarization, by an unknown mechanism, probably hydrogen embrittlement;

c. In "pure" methanol, by a mechanism involving either catalytic dehydrogenation of the methanol at the metal surface, or by a corrosion reaction between titanium and methanol to form the methoxide, probably the latter;

d. In methanol-carbon tetrachloride mixtures, by a mechanism similar to (a);

e. In nonaqueous solvents containing dissolved bromine, by a "pure" corrosion reaction between the metal and bromine; and

f. In liquid mercury, by a stress-sorption process.

REFERENCES

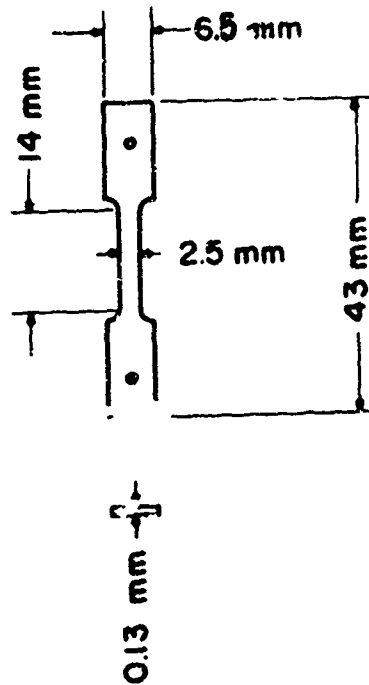
1. M. G. Fontana, Ind. and Eng. Chem., 1956, 48, 91.
2. B. F. Brown, Materials Res. and Standards, 1966, 6, 129.
3. K. Mori, A. Takamura and T. Shimose, Corrosion, 1966, 22, 29.
4. A. J. Sedriks, J. A. Green and R. W. Slattery, Corrosion, 1968, 24, 172.
5. A. J. Sedriks, Corrosion, 1969, 25, 207.
6. E. G. Haney, W. R. Wearmouth, G. Goldbery, R. F. Ernsberger and W. T. Brehm, Semiannual reports No. 1, November 1966 and No. 3, November 1967, Mellon Inst., Pittsburgh, Pa.
7. T. R. Beck, J. Electrochem. Soc., 1967, 116, 551.
8. T. R. Beck, Quarterly progress reports No. 1, July 1966, No. 6, December 1967, Boeing Scientific Res. Lab., Seattle, Washington.
9. G. Sanderson and J. C. Scully, Corrosion Science, 1966, 6, 541.
10. D. T. Powell and J. C. Scully, Corrosion, 1968, 24, 151.
11. H. L. Gegel, H. B. Kirkpatrick and C. M. Swinning, Corrosion, 1969, 25, 215.
12. M. Levy and D. W. Seitz, Tech. Report No. AMMRCTR-68-21, D/A Proj. 7Co2440/A328, November 1968.
13. C. M. Chen, F. H. Beck and M. G. Fontana, Corrosion (to be published).
14. G. Sandoz, Proceedings of Conference, Fundamental Aspects of Stress Corrosion Cracking, 1969, Ohio State Univ. (N.A.C.E.) p. 684.
15. A. J. Sedriks, Corrosion, 1969, 25, 207.
16. G. Sanderson and J. C. Scully, Corrosion Science, 1968, 8, 541.
17. I. A. Menzies and A. F. Averill, Electrochimica Acta, 1968, 13, 807.

REFERENCES (Cont'd)

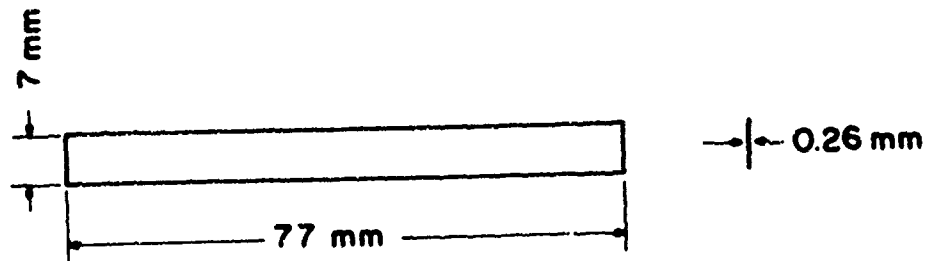
18. N. D. Tomashov, R. M. Altovskiy and V. B. Vladimirov, Translation FTD-TT-63-672/1+2, pp 221-233a, Translation Division, Foreign Technology Division, Wright-Patterson Air Force Base, Ohio.
19. F. H. Cocks, A.S.T.M., 1969, 9, 29.
20. E. G. Haney and W. R. Wearmouth, Corrosion, 1969, 25, 87.
21. A. J. Sedriks and J.A.S. Green, Corrosion, 1969, 25, 324.
22. A. J. Sedriks, P. W. Slattery and E. N. Pugh, Proceedings of Conference, Fundamental Aspects of Stress Corrosion Cracking, 1969, Ohio State Univ. (N.A.C.E.) p. 673.
23. J. R. Ambrose and J. Kruger, Corrosion Science, 1969, 8, 119.
24. E. G. Haney et al., Progress Reports No. 2 and No. 4, NASA Research Grant NGR-39-008-014.
25. M. G. Fontana, Air Force Materials Laboratory Technical Reports, Contract No. F33615-69-C-1258, June 1968-May 1970, Ohio State Univ., Columbus, Ohio.
26. H. L. Gegel and S. Fujishiro, J. Less-Common Metals, 1969, 17, 305.
27. L. R. Leith, Joe W. Hightower and C. G. Harkins, Corrosion (To be published).
28. S. Kishimoto, J. Phys. Chem., 1962, 66, 2694.
29. I. Uhara, S. Yanagimoto, G. A. Adachi and S. Teratani, J. Phys. Chem., 1962, 66, 2691.
30. T. R. Beck and M. J. Blackburn, AIAA Journal, 1968, 6, 326.
31. K. E. Weber, J. S. Fritzen, D. S. Cowgill, and W. C. Gillchriest, "Accelerated Crack Propagation of Titanium by Methanol, Halogenated Hydrocarbons, and Other Solutions", DMIC Memorandum 228, 6 March 1967, p. 39.

REFERENCES (Cont'd)

32. W. S. DeForest, paper presented at the Western Regional Meeting of N.A.C.E. San Diego, California, September 1968.
33. R. L. Horst, Jr., E. H. Hollingsworth and W. King, Corrosion, 1969, 25, 199.
34. F. H. Cocks, J. F. Russo and S. B. Rummer, Corrosion, 1968, 24, 206.
35. D. N. Fager and W. F. Spurr, Transaction of A.S.M., 1968, 61, 283.
36. D. A. Mauney and E. A. Starke, Jr., Corrosion, 1969, 25, 177.
37. C. M. Chen and H. B. Kirkpatrick, Corrosion, 1970, 12, 539.



Tensile Specimen for Straining Electrode Tests



Bend Specimen for Static Tests

Figure 1a. Specimen Configurations

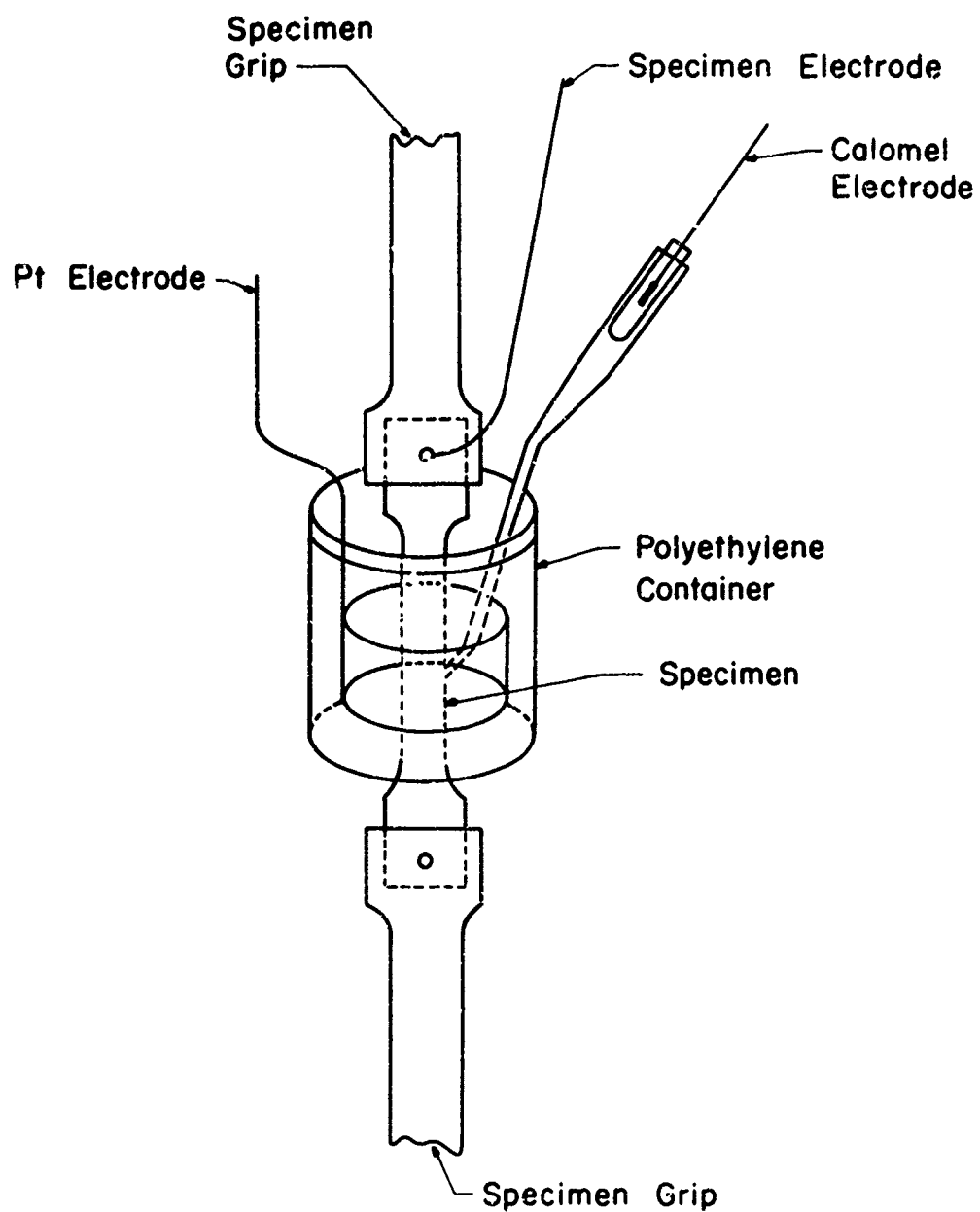


Figure 1b. Cell for Straining Electrode Tests

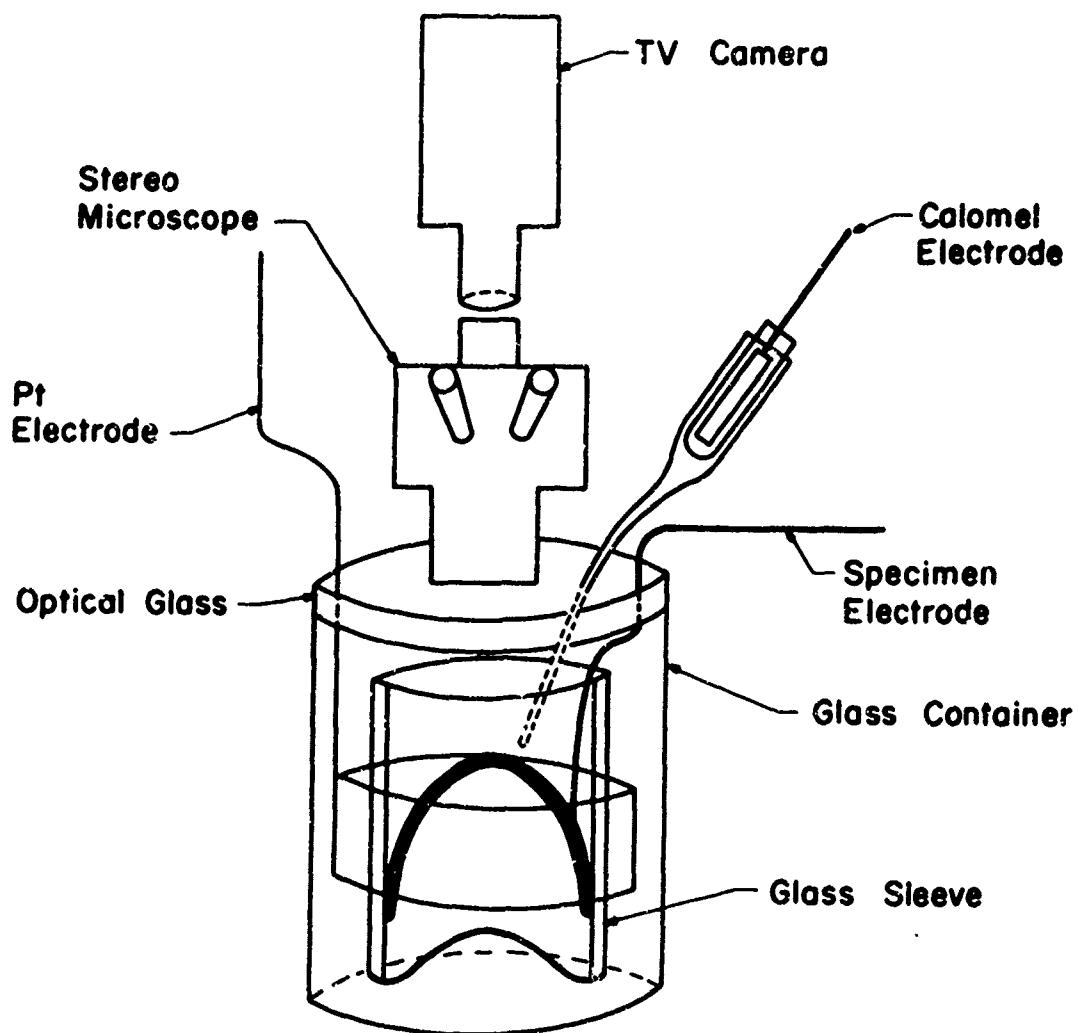
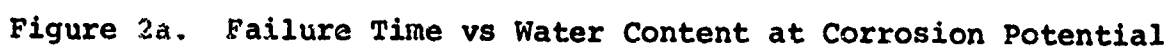


Figure 1c. Cell for Stress Corrosion Bend Tests



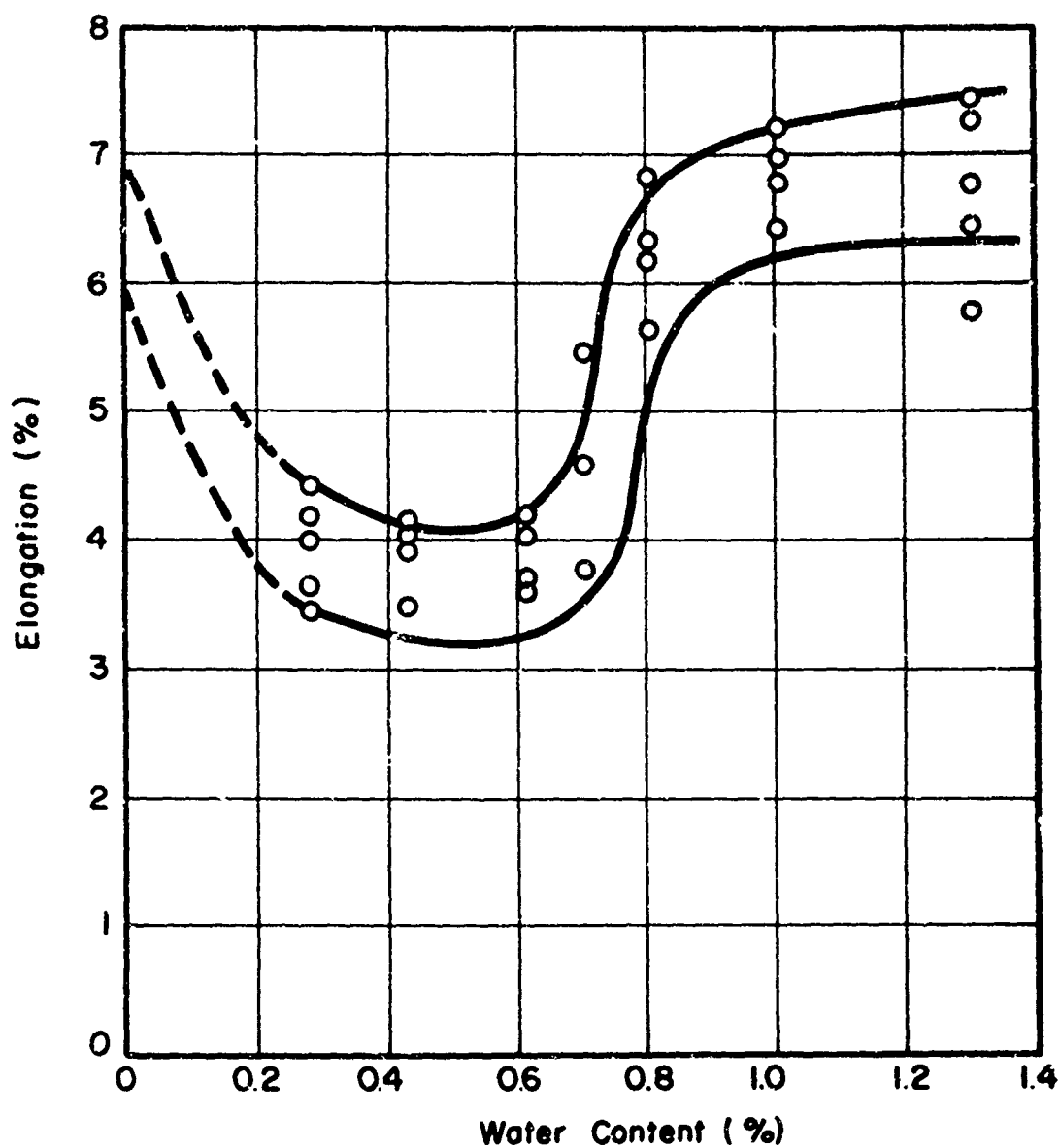


Figure 2b. Elongation vs Water Content: $\text{CH}_3\text{OH} + 0.166\% \text{HCl} + \text{H}_2\text{O}$ (Tensile Direction Parallel to Rolling Direction; Strain Rate 0.005 cm/min)

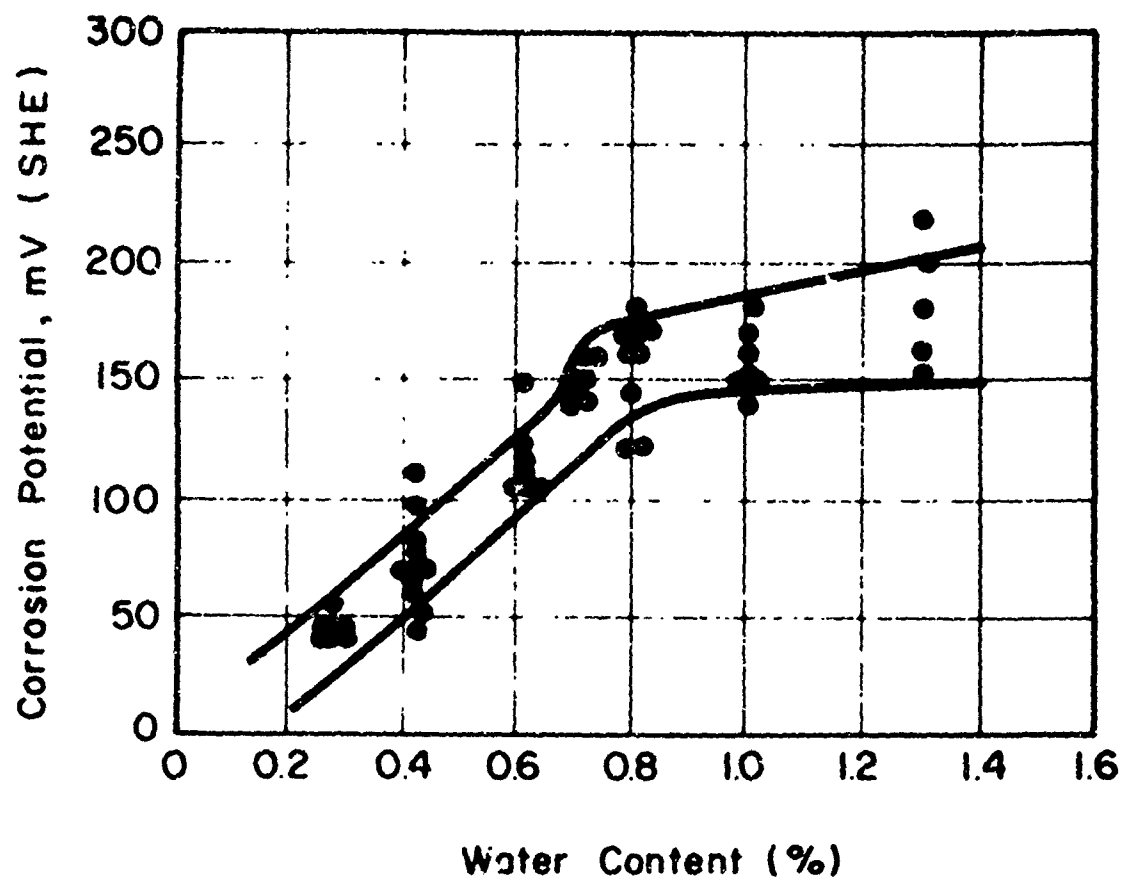


Figure 3. Corrosion Potential vs Water Content; $\text{CH}_3\text{OH} + 0.166\% \text{HCl} + \text{H}_2\text{O}$ (No Applied Load)

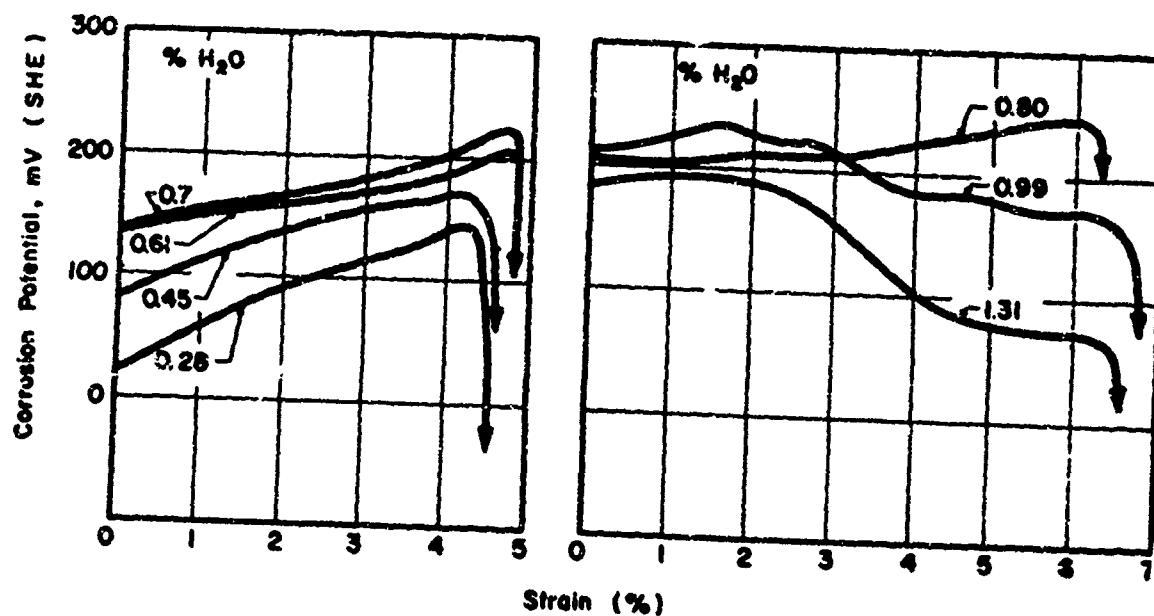


Figure 4. Corrosion Potential vs Elongation in CH₃OH + 0.166% HCl + H₂O

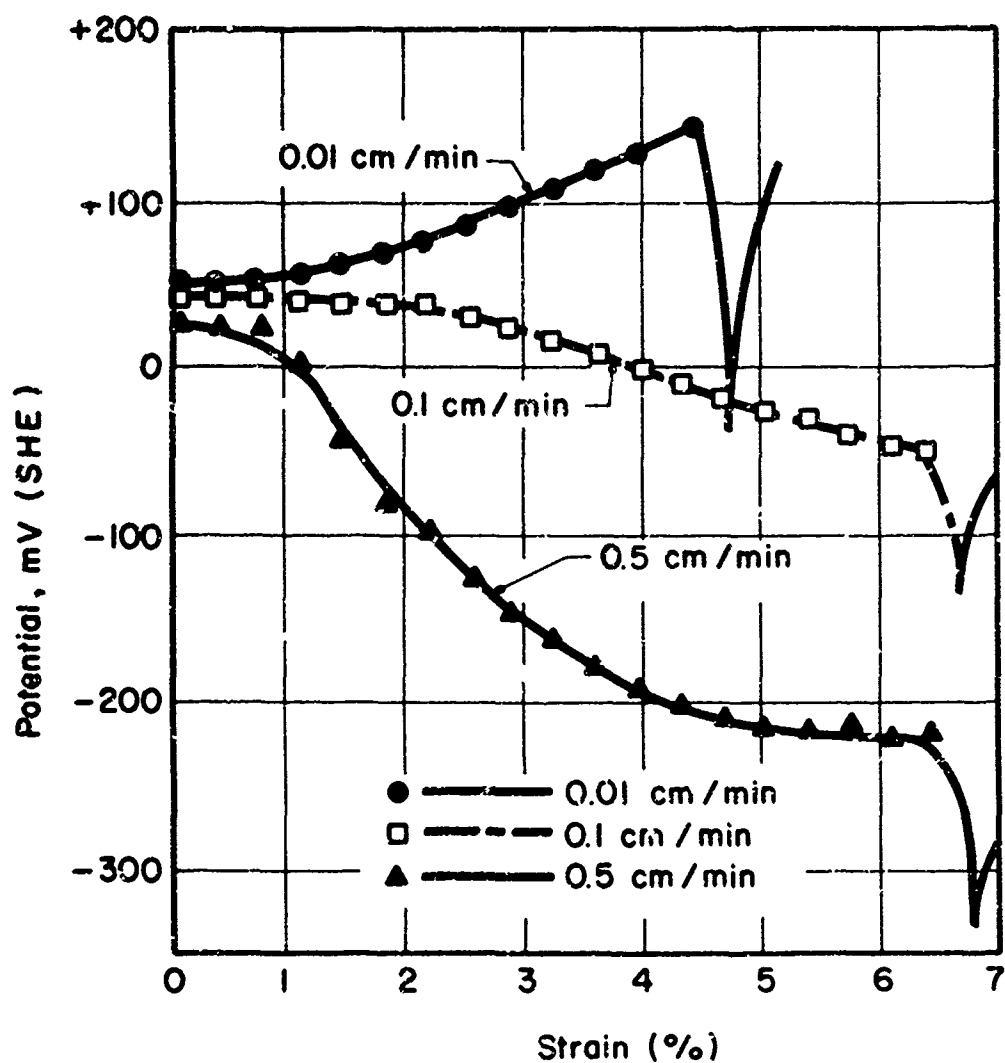


Figure 5a. Effect of Strain Rate on Corrosion Potential vs Strain in $\text{CH}_3\text{OH} + 0.166\% \text{HCl} + 0.28\% \text{H}_2\text{O}$

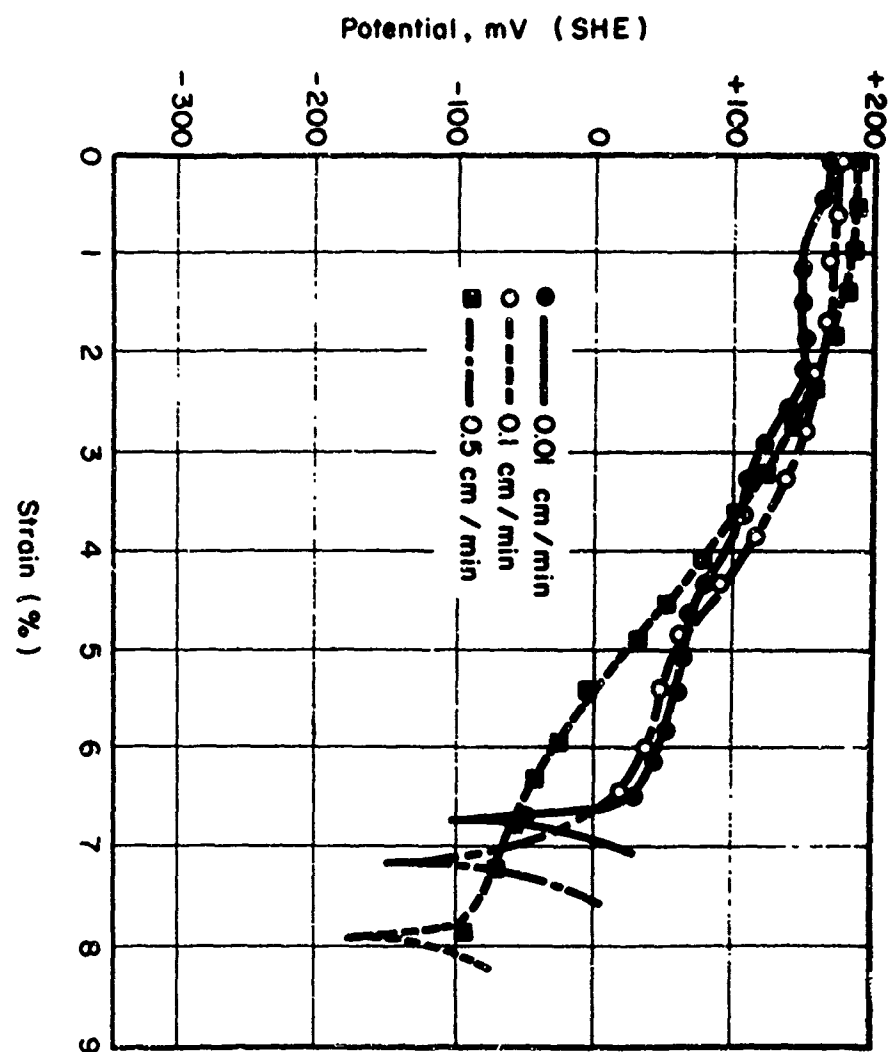


Figure 5b. Effect of Strain Rate on Corrosion Potential vs Strain in $\text{CH}_3\text{OH} + 0.166\% \text{ HCl} + 0.99\% \text{ H}_2\text{O}$

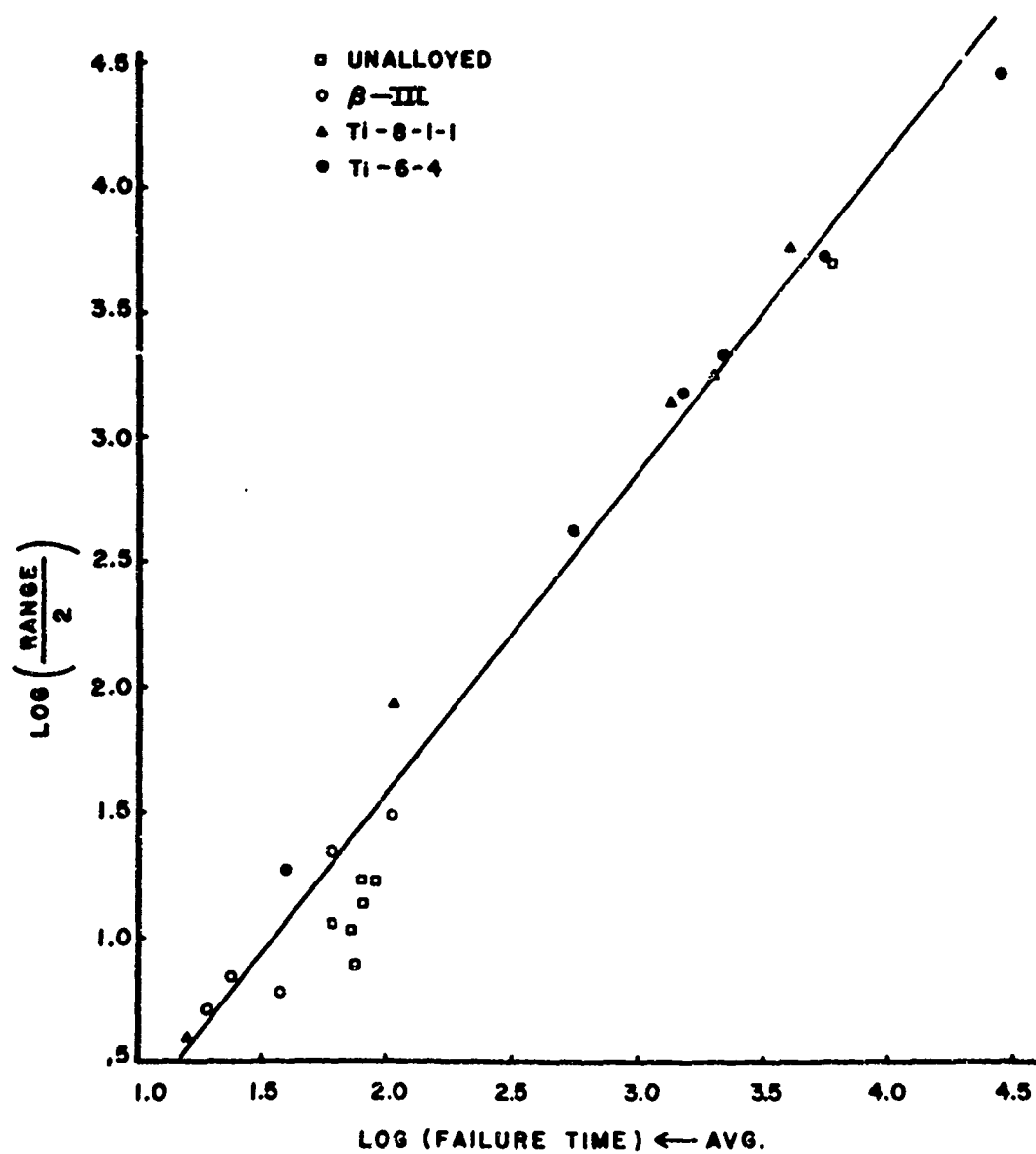


Figure 6. Half-Range of Scatter in Failure Time vs Average Failure Time

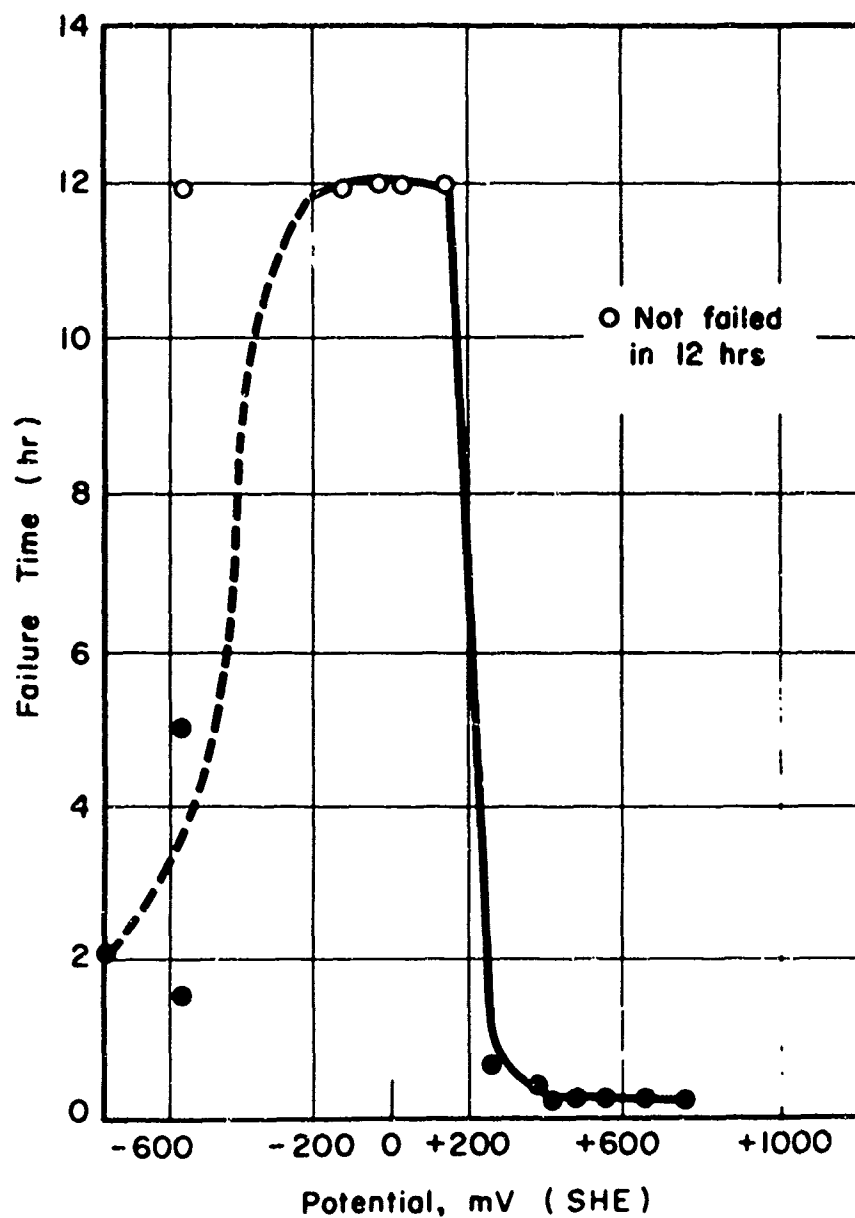


Figure 7. Failure Time vs Polarization Potential in CH_3OH + 0.166% HCl + 0.99% H_2O

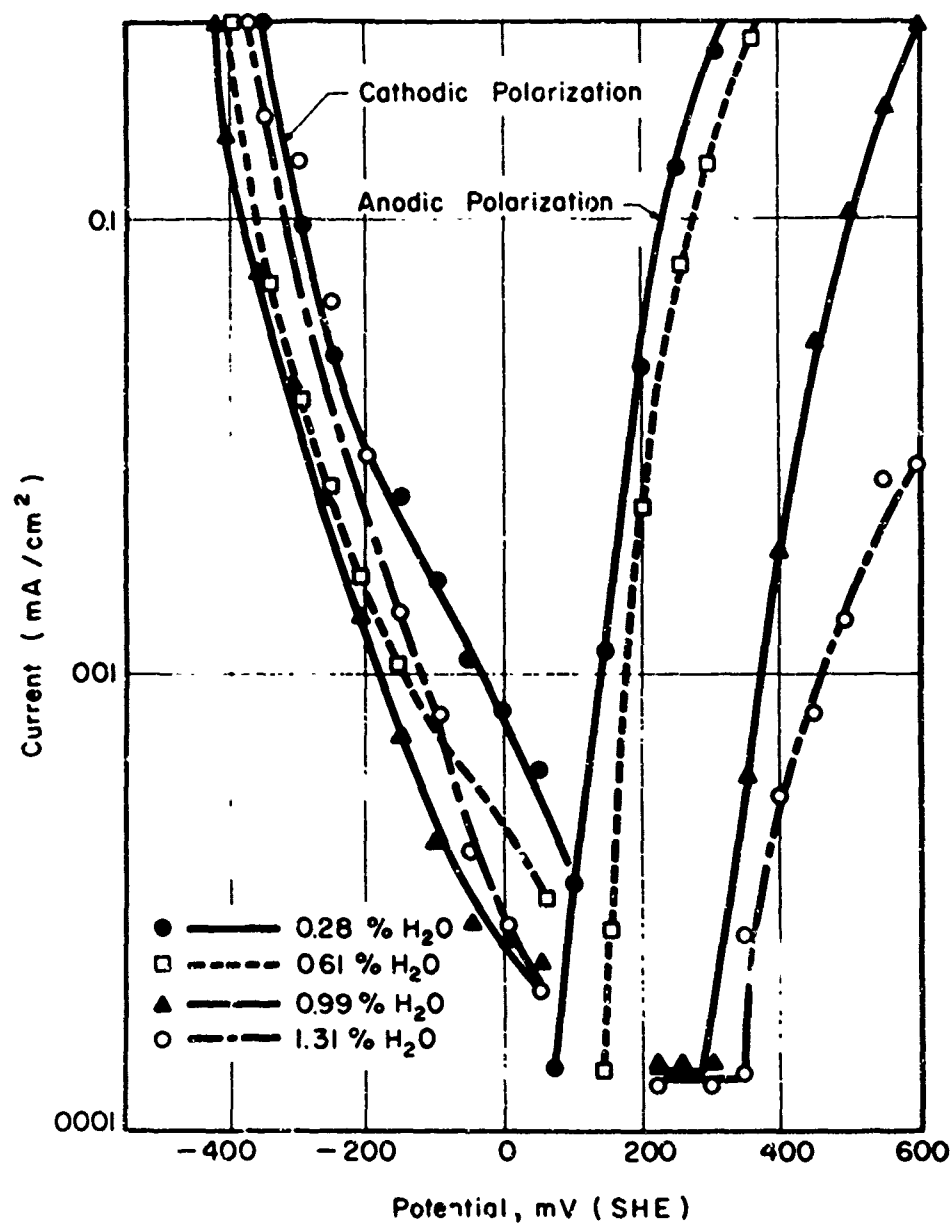
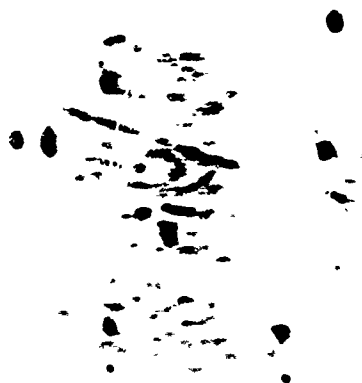


Figure 8. Effect of Water Content on the Polarization Curves in $\text{CH}_3\text{OH} + 0.166\% \text{HCl} + \text{H}_2\text{O}$ (Scanning rate 25 mV/min)



Before Polarization



After About Two Minutes Polarization



After About Six Minutes Polarization

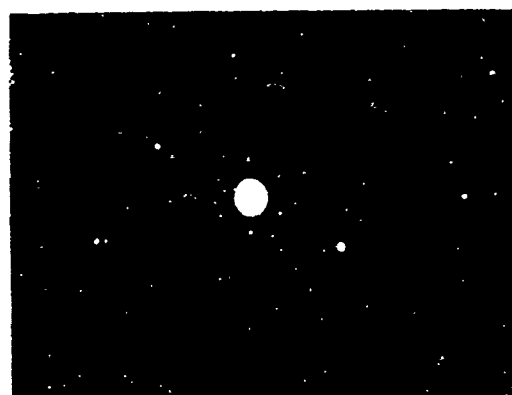
Figure 9. Pitting and Crack Formation of Ti-6Al-4V Alloy in $\text{CH}_3\text{OH} + 0.17\% \text{HCl} + 1\% \text{H}_2\text{O}$, Under Polarization of +450 mV (SHE). (Approx 400X. Tensile Axis of U-Bend in Direction of Television Scan Lines)



(a) External Surface



(b) Fracture Surface



(c) Electron Diffraction Pattern of Corrosion Product (TiCl_3)

Figure 10. Corrosion Products on External and Fracture Surfaces of Ti-6Al-4V Fractured in $\text{CH}_3\text{OH} + 0.17\% \text{HCl} + 1\% \text{H}_2\text{O}$ (Carbon Replica; X2,350) (a) External Surface; (b) Fracture Surface; (c) Electron Diffraction Pattern of Corrosion Product (TiCl_3)

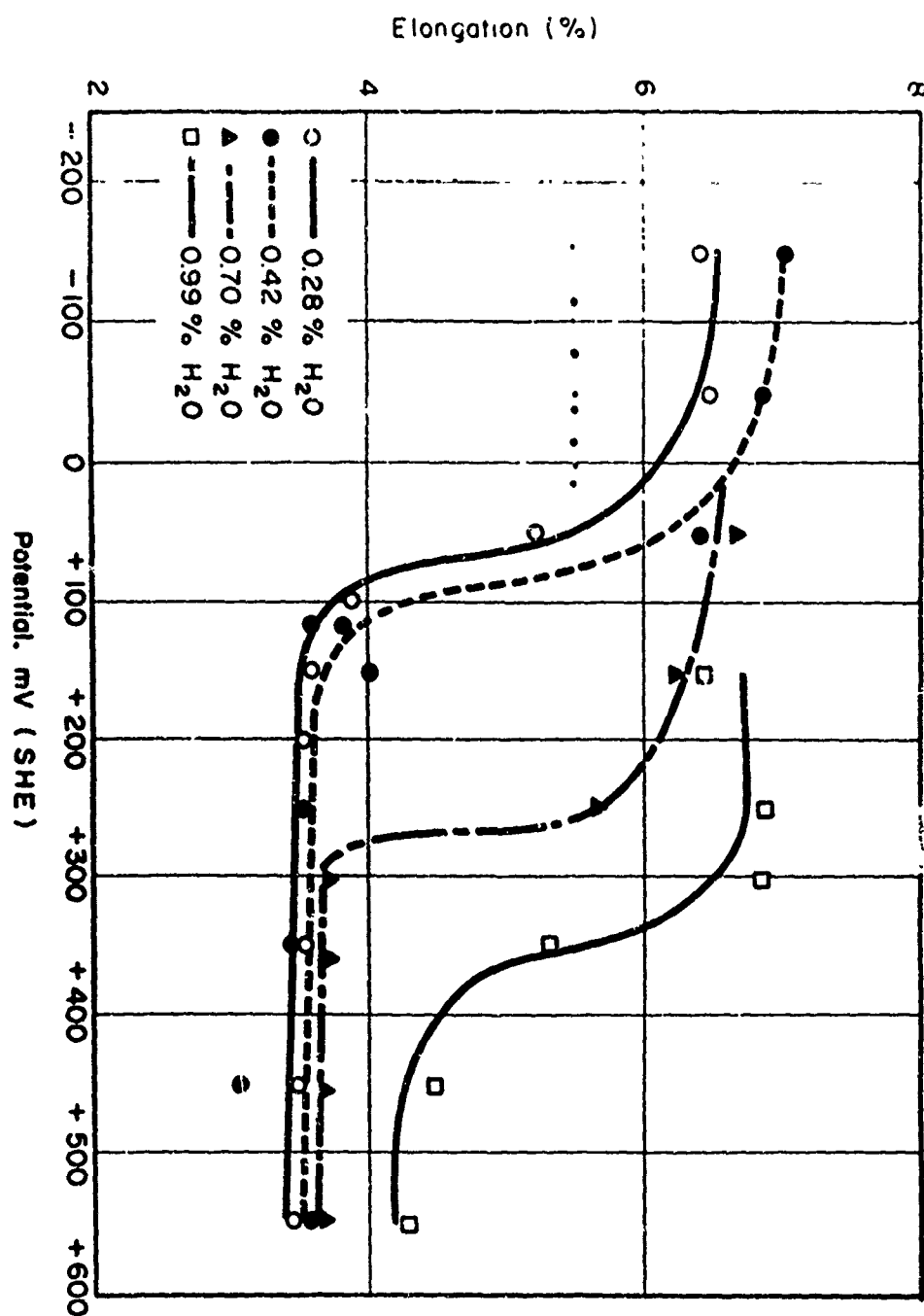


Figure 11. Effect of Polarization Potential on Elongation

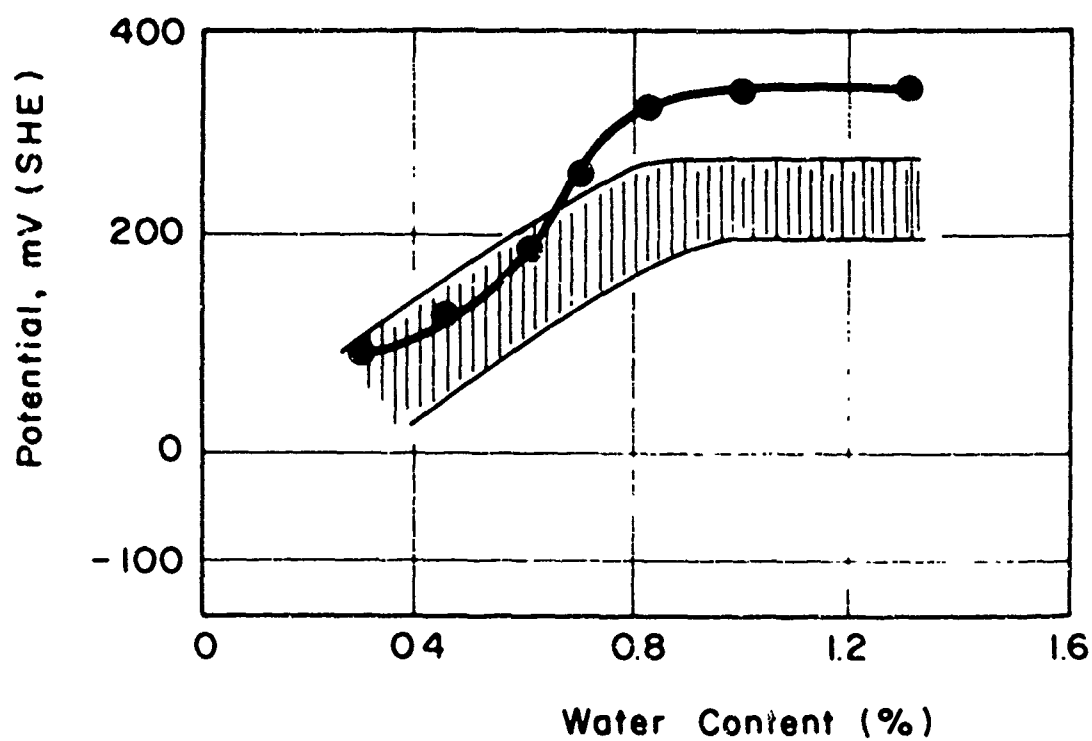


Figure 12. Transition Potential vs Water Content

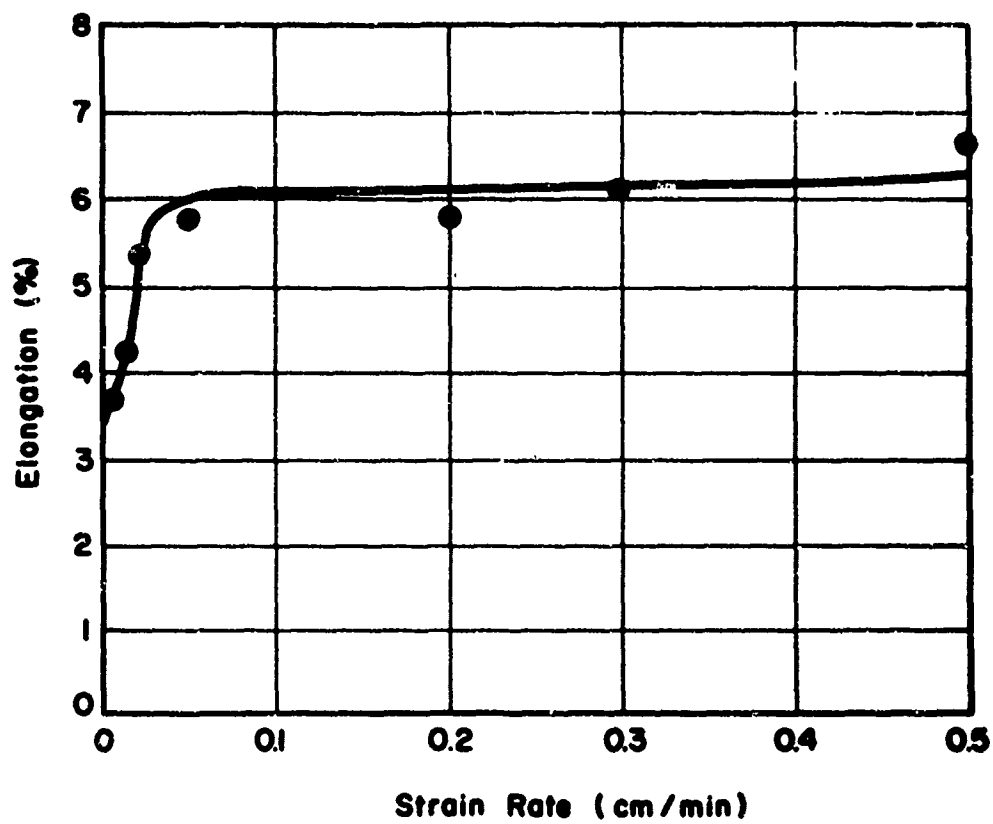


Figure 13a. Effect of Strain Rate on Specimen Elongation at +350 mV (SHE)

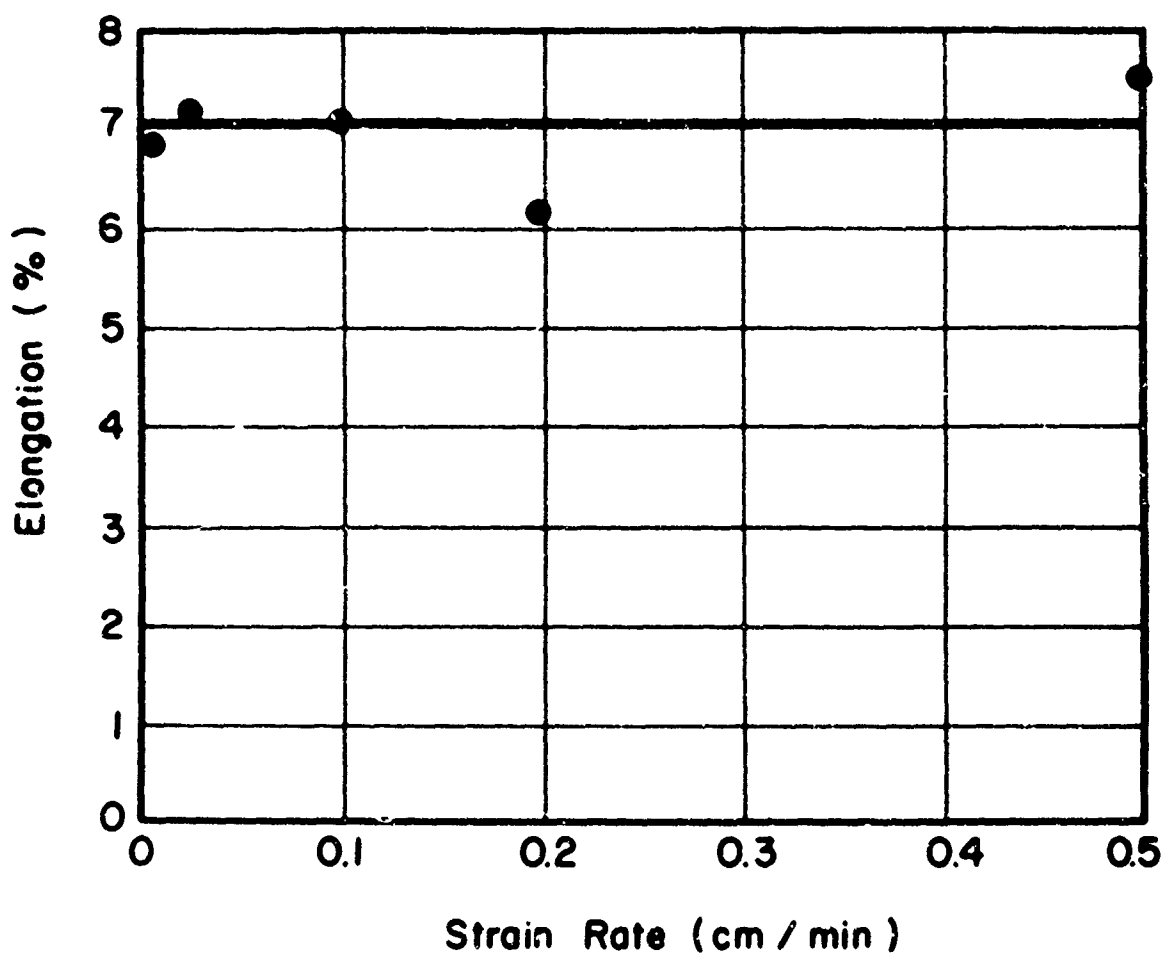


Figure 13b. Effect of Strain Rate on Specimen Elongation at +50 mV (SHE)

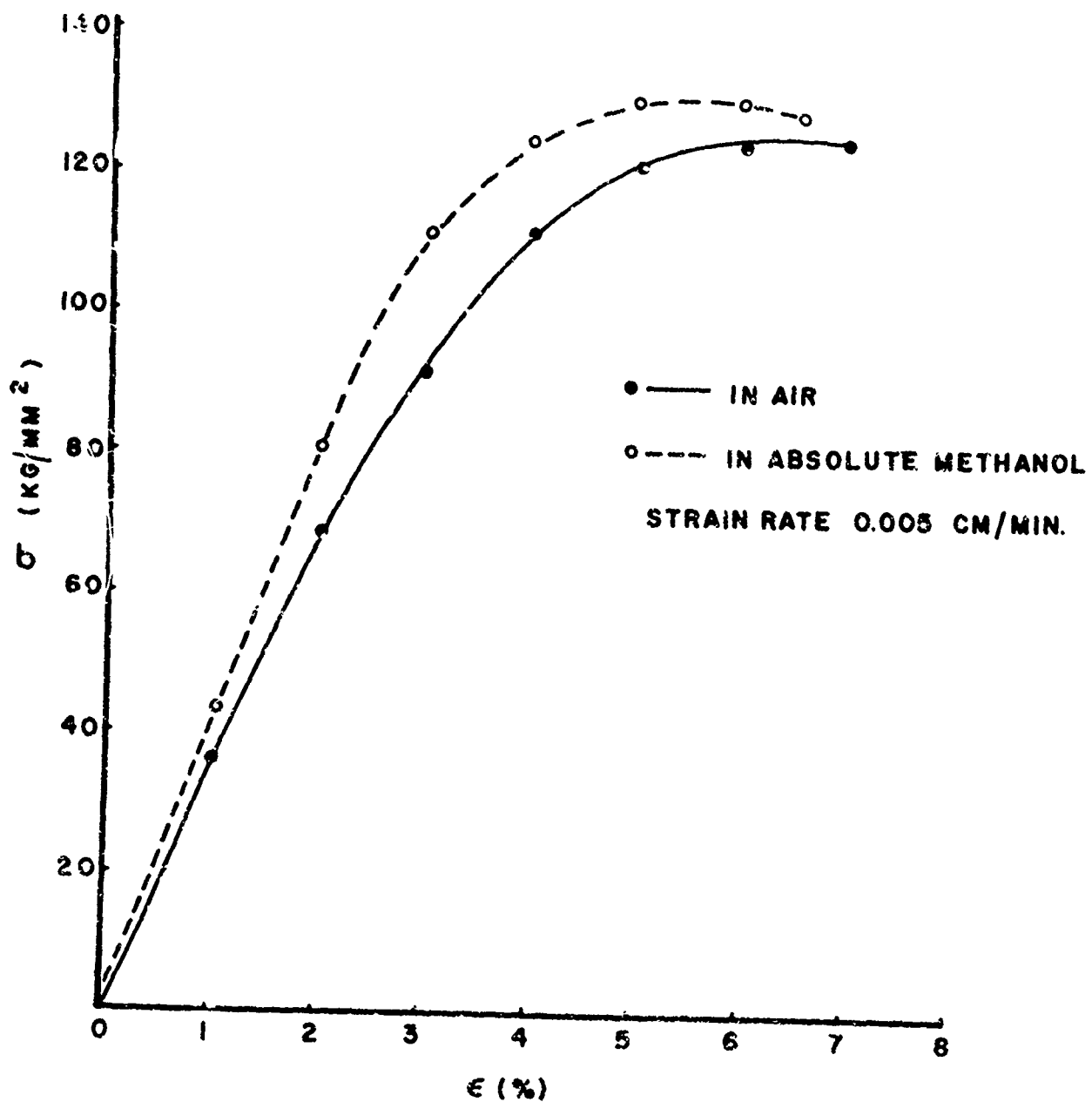


Figure 14. Stress-Strain Curves of Ti-6Al-4V in Air and in Absolute Reagent Grade Methanol (0.015% H₂O)

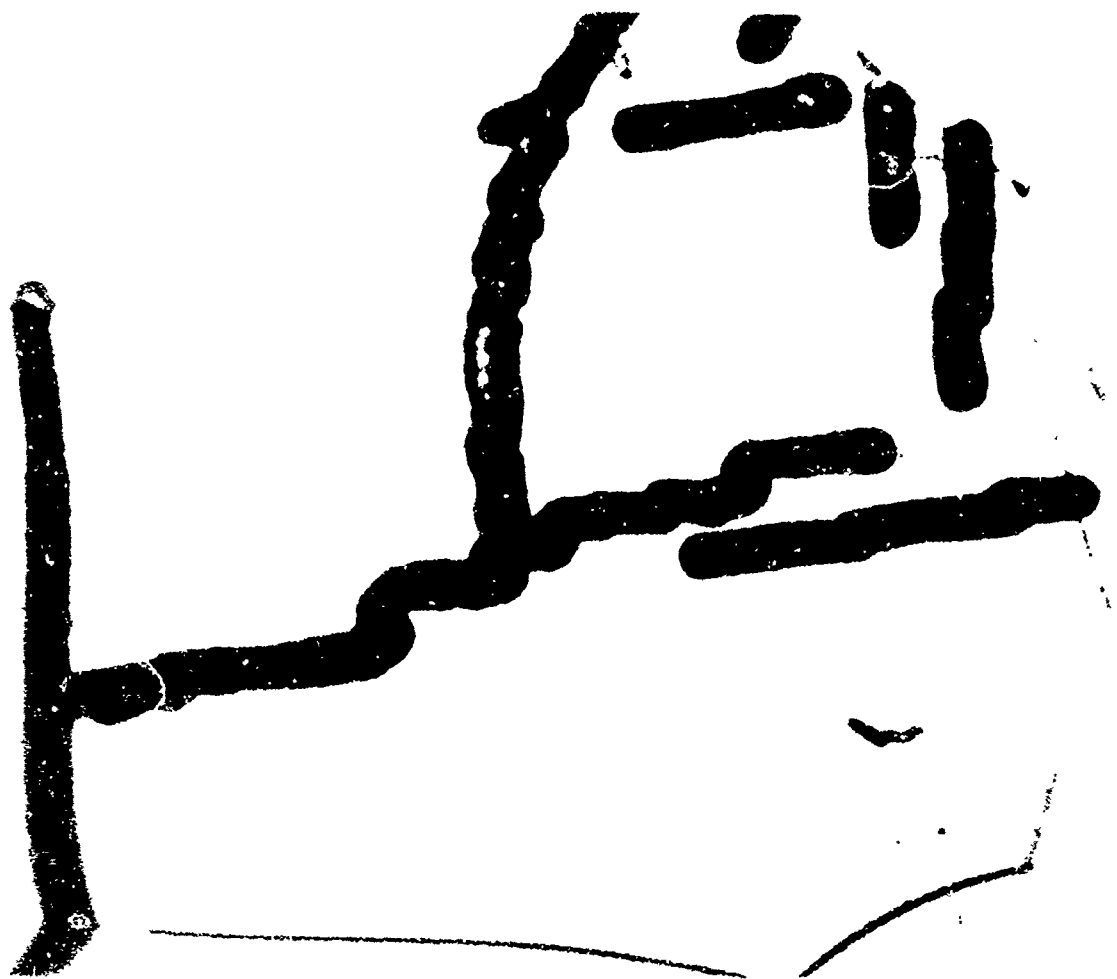


Figure 15. Transgranular Stress Corrosion Cracking of Heat-Treated 8-III Alloy in Methanol Vapor

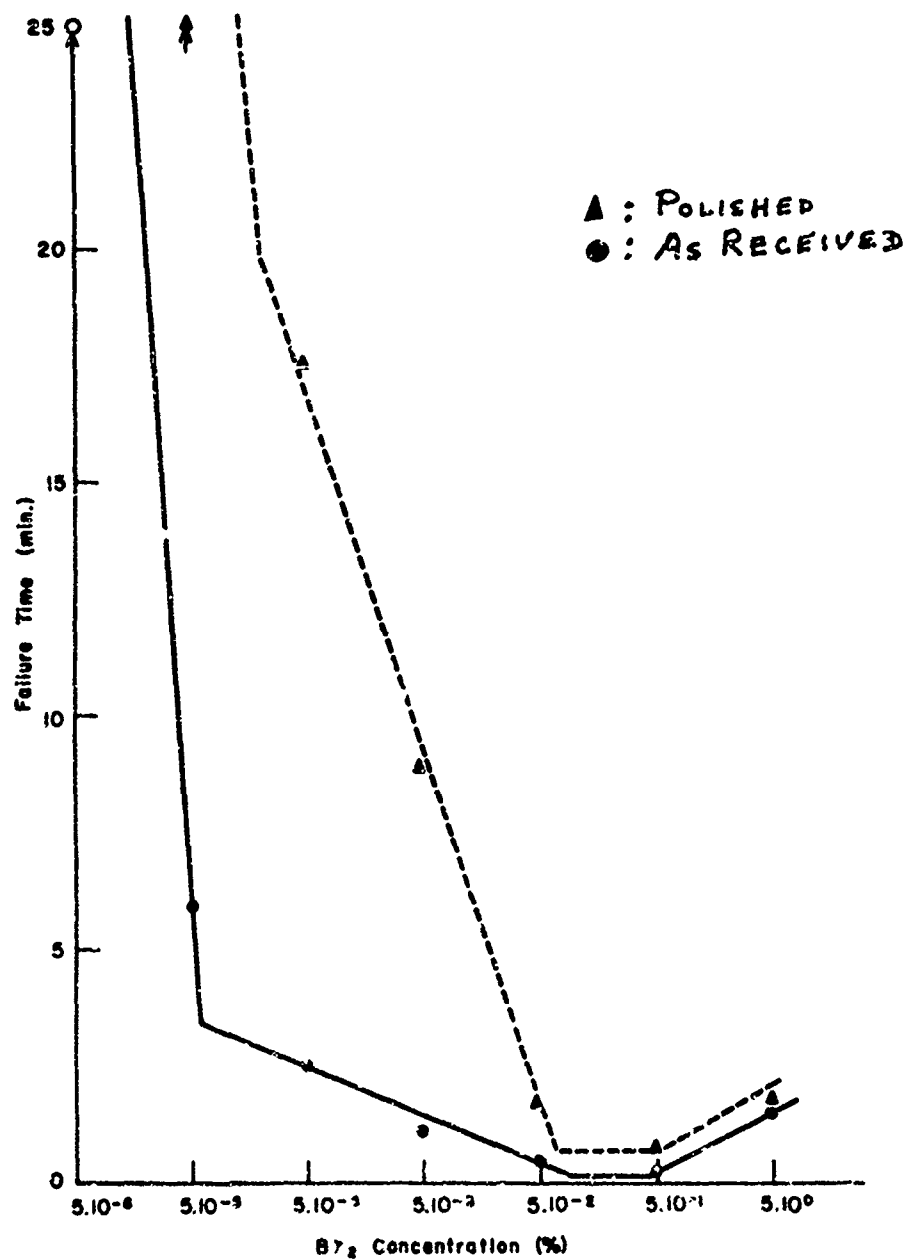


Figure 16a. Failure Time vs Bromine Concentration: Titanium
 8-1-1

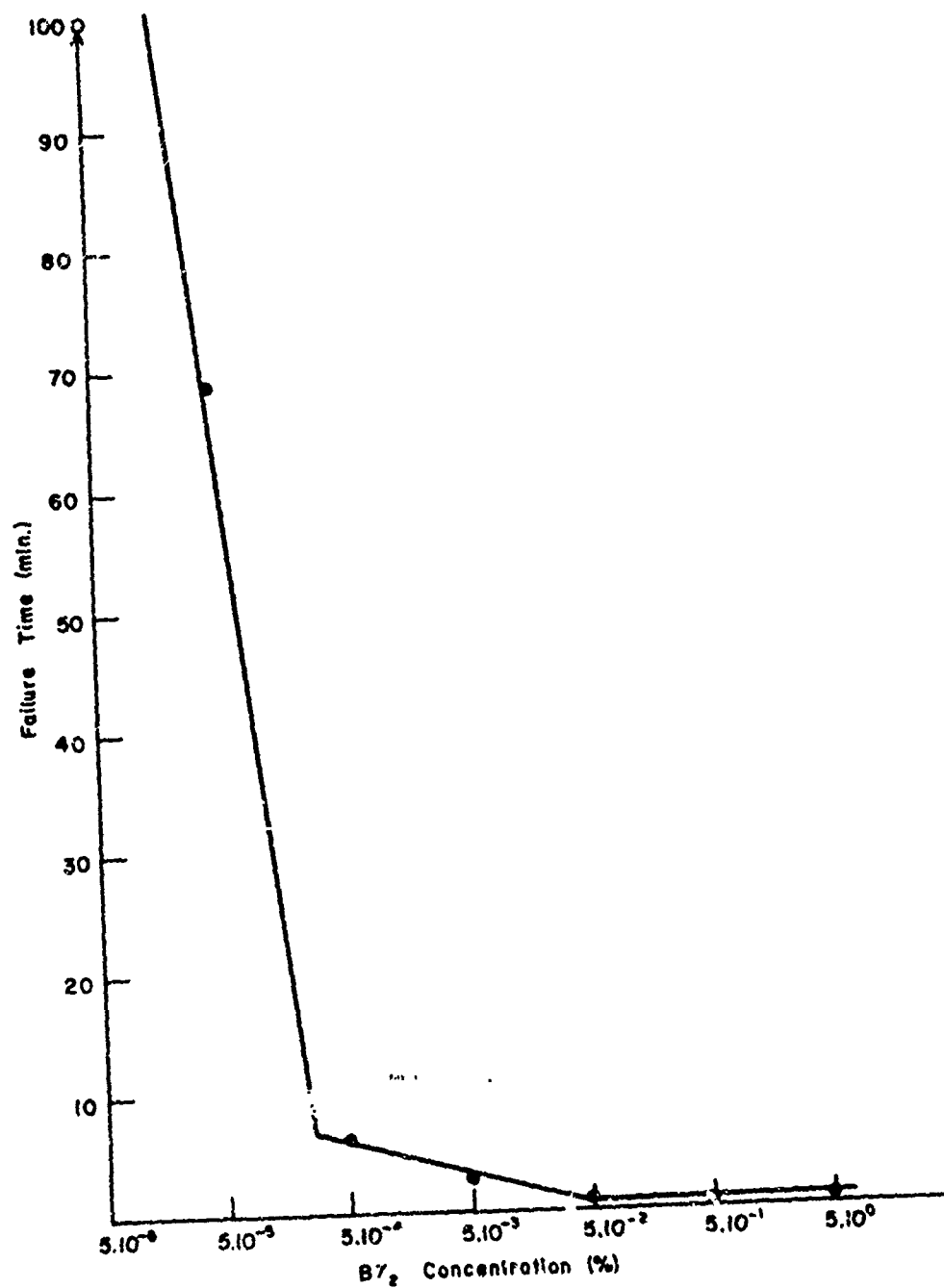


Figure 16b. Failure Time vs Bromine Concentration; Heat-Treated β -III

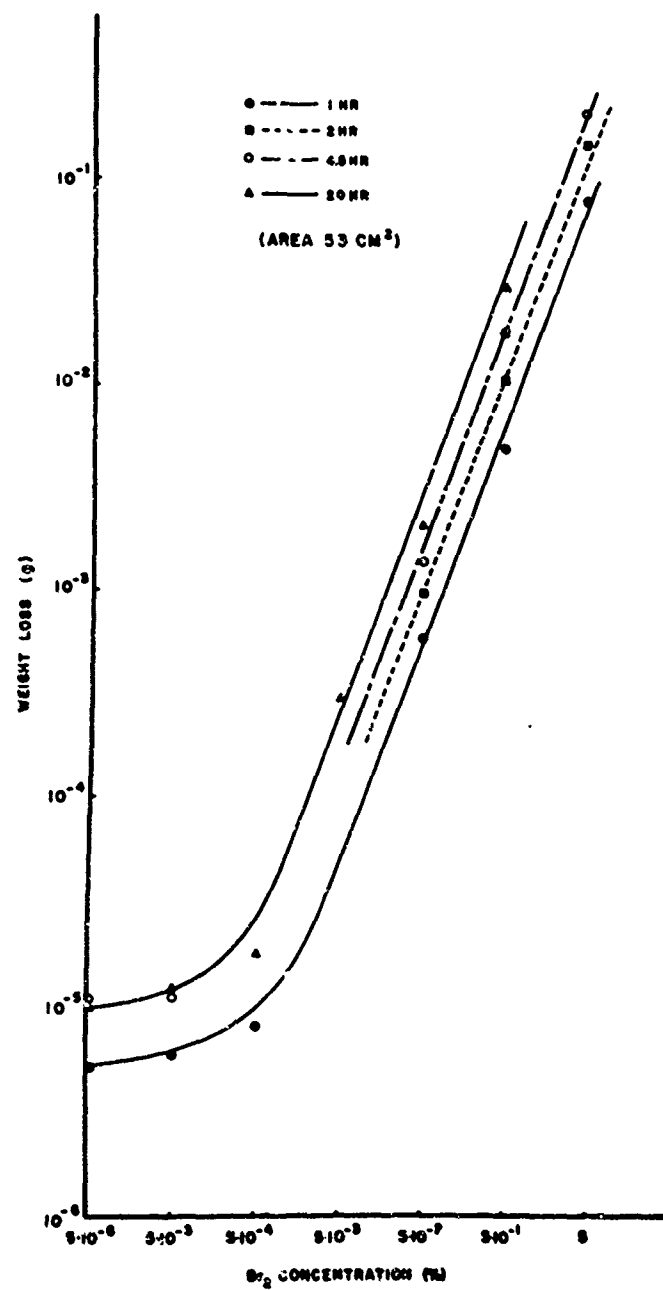
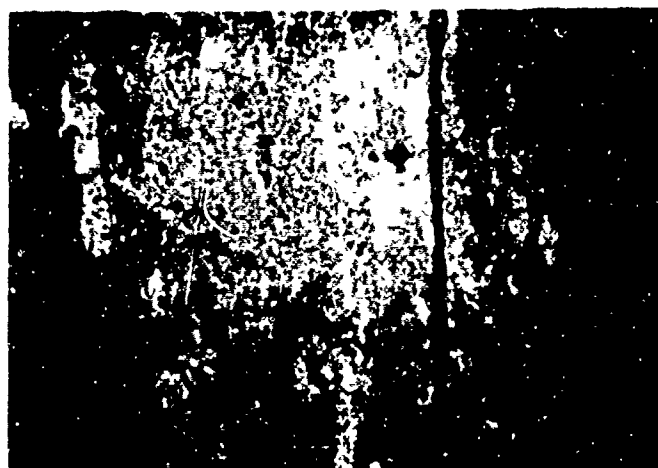
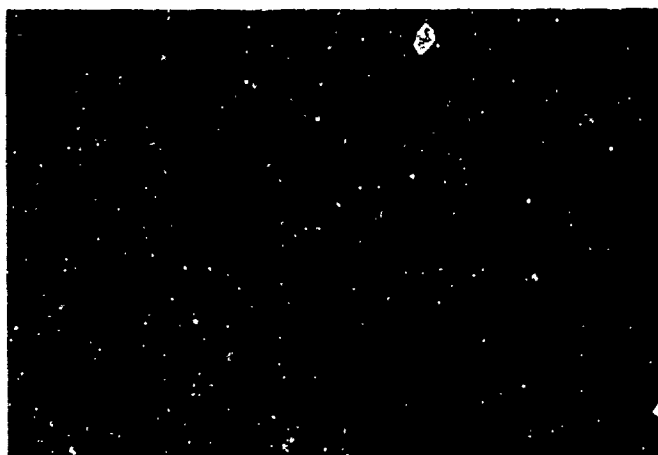


Figure 17. Weight Loss vs Bromine Concentration; Titanium 8-1-1



(a) Tensile Direction Perpendicular to Rolling Direction



(b) Tensile Direction at 45° to Rolling Direction



(c) Tensile Direction parallel to Rolling Direction

Figure 18. Stress Corrosion Cracking of Ti-8Al-1Mo-1V Alloy in CH_3OH ; 0.5% Bromine Solution (X50)

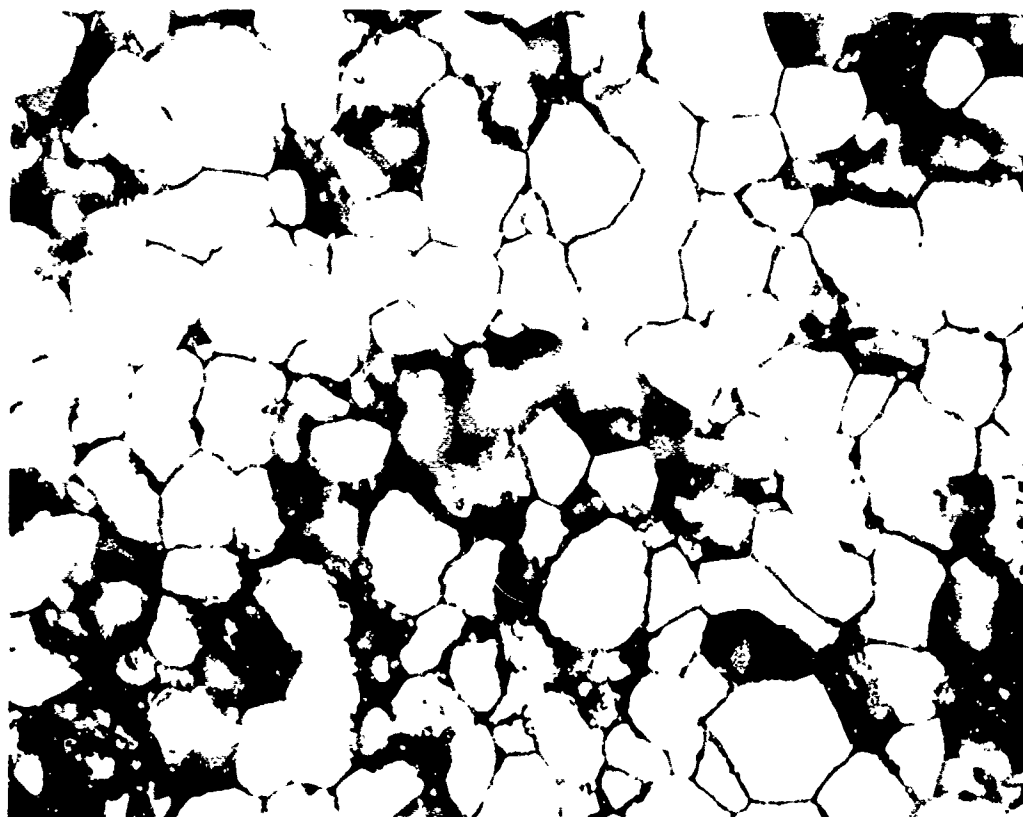


Figure 19. Intergranular Corrosion of Unalloyed Titanium (RMI70) in Bromine-Methanol Solution (1%Br₂; 68-Hour Exposure; No External Stress; X300)

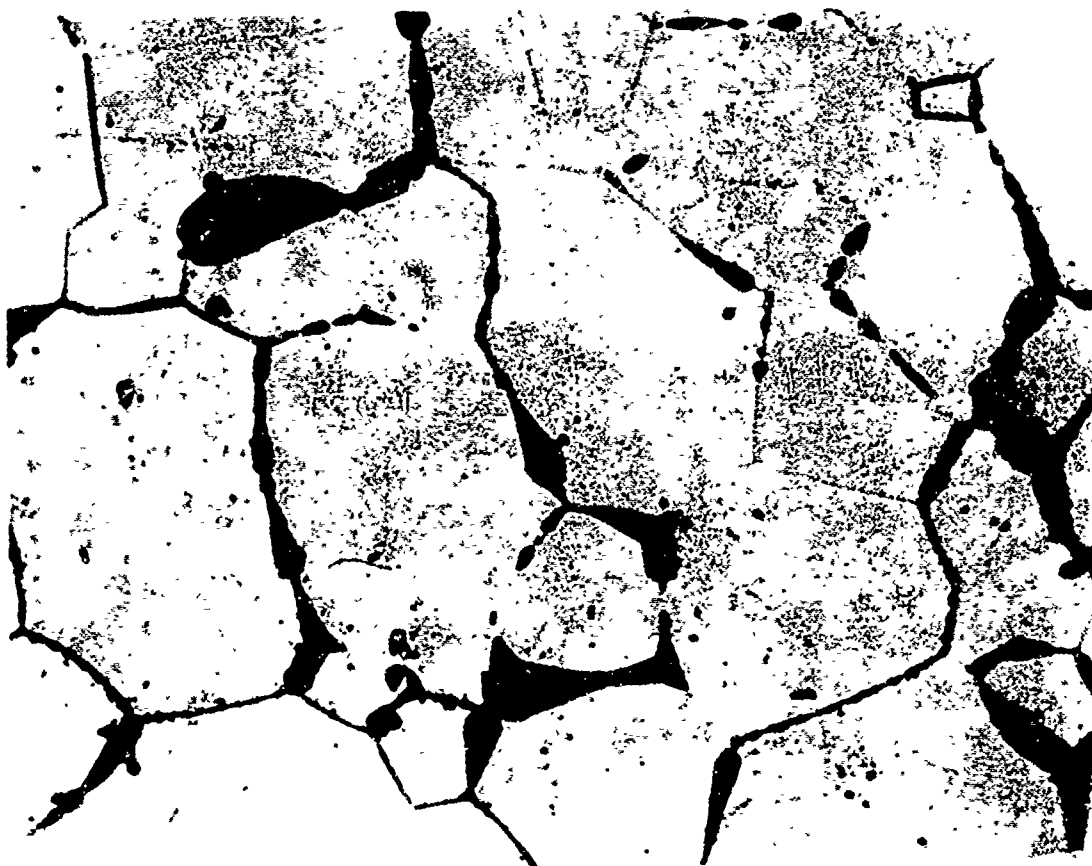


Figure 20. Grain Boundary Corrosion Near Center of Heat-Treated B-III Alloy Specimen in Bromine-Methanol Solution (0.05%Br₂; 164 Hours; No External Stress; X210)

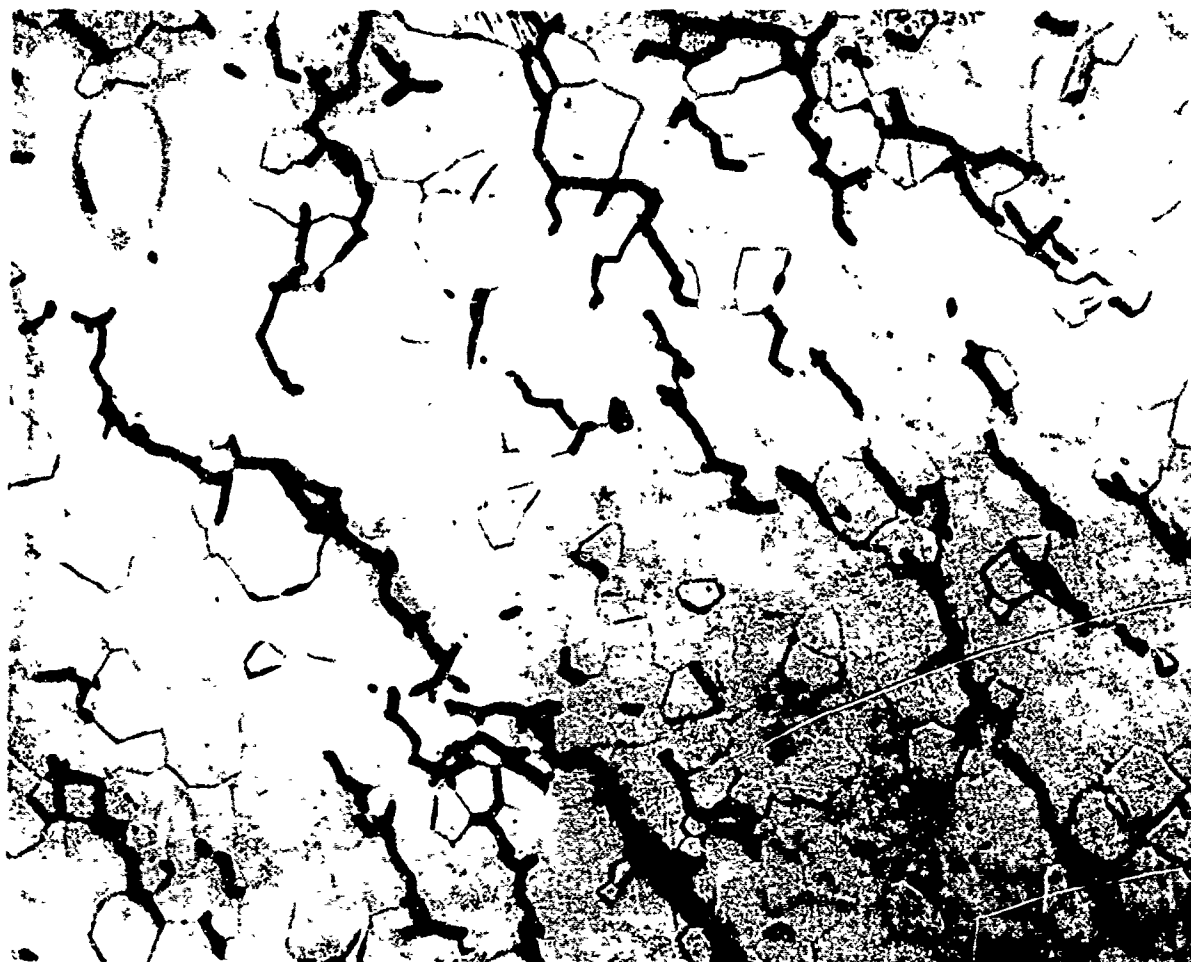


Figure 21. Stress Corrosion Cracking of Heat-Treated β -III Alloy in Bromine-Methanol Solution ($0.5\% \text{Br}_2$; X50)

Reproduced from
best available copy.



Figure 22. Stress Corrosion Cracking From Residual Stress at Edge of β -III Specimen ($0.05\%Br_2$; X150)



Figure 23. Transgranular Cracking of Highly Stressed β -III Alloy in Bromine-Methanol Solution (Note relationship of crack direction to slip lines caused by plastic deformation.)

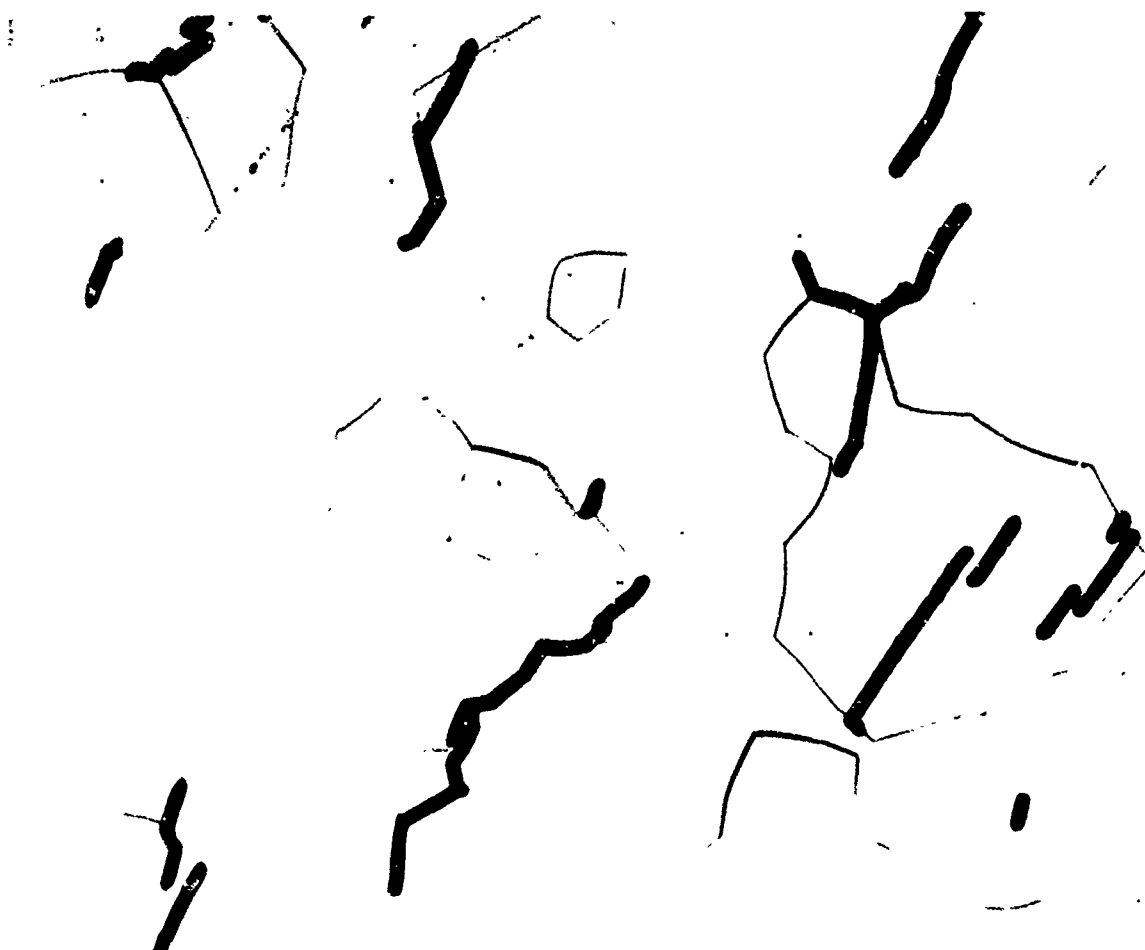


Figure 24. Stress Corrosion Cracking of Heat-Treated 8-III Alloy in $\text{CH}_3\text{OH} + 0.17\%\text{HCl} + 0.28\%\text{H}_2\text{O}$ (X100)